Chemical Reviews

Volume 86, Number 6 December 1986

Absorption Spectroscopy of Sandwich Dimers and Cyclophanes

JAMES FERGUSON

Research School of Chemistry, Australian National University, Canberra, A.C.T. 2601, Australia

Received January 29, 1986 (Revised Manuscript Received June 27, 1986)

Contents

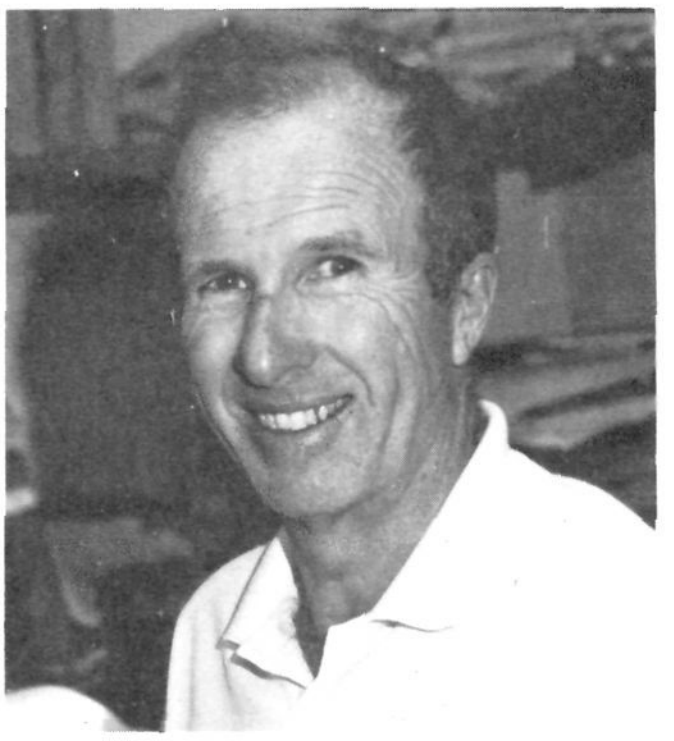

James Ferguson was born in Sydney, Australia, in 1931. He obtained his Ph.D. degree from the University of Sydney in 1956, and then he was a NRC postdoctoral fellow in Ottawa with W. G. Schneider. After holding positions in the University of British Columbia, CSIRO (twice), and the Bell Laboratories (Murray Hill), he moved to a professorial fellowship (equivalent to associate professor or reader) in the Research School of Chemistry at the ANU in 1970. After 16 years in that position he has decided to take early retirement late in 1986. His research interests cover the spectroscopy and photochemistry of organic and inorganic compounds in condensed phases, particularly crystalline media.

I. Introduction

The term sandwich dimer originally referred to a pair of planar aromatic chromophores, obtained by photolytic cleavage, which are constrained by their environment to adopt a face-to-face arrangement.[1] The first example was given by Chandross[2] who photocleaved dianthracene in methylcyclohexane at 77 K and obtained "pairs of anthracene molecules which are forced to remain close together by the matrix". Chandross noted the presence of a broad structureless fluorescence with maximum intensity about 480 nm.

At the same time the author was examining the controlled softening of rigid glass solutions of aromatic molecules to see whether dimers could be obtained under such conditions. Anthracene was found to form a dimer but its spectral characteristics are quite different from those of Chandross' dimer. It was called a stable dimer and the spectroscopic features of both dimers were analyzed[3] using a vibronic coupling model developed by Fulton and Gouterman.[4] Sandwich dimers of substituted anthracenes were also studied.[5]

Although the sandwich dimer of anthracene is not stable, i.e., on softening of the solvent cage it dissociates, there are some aromatic molecules which adopt a parallel sandwichlike pair arrangement in their crystal

0009-2665/86/0786-0957$06.50/0

structures. If the solubility is low enough, then stable sandwich dimers can be obtained by controlled softening of glassy solutions. Perylene is an example.[6] Stevens[7] noted that all crystals containing sandwichlike pairs (type B) give rise to fluorescence with a very pronounced red shift (Stokes shift), whereas the remaining crystals, with a monomer unit (type A), have their fluorescence spectra in a normal mirror image relation to the absorption spectra. Since the classification by Stevens[7] it has been found that many aromatic compounds exist in both crystal modifications, e.g., perylene which has α (type B) and β (type A) forms.[8] Although both forms can be obtained by crystallization from hydrocarbon solutions, the β form reverts to the α form at 140 °C.[8] The formation of the sandwichlike stable dimer by controlled softening of a rigid hydrocarbon glass is consistent with the greater stability of the α crystal form.[6]

The large Stokes shift of the fluorescence from type B crystals, initially observed for pyrene,[9] is an example of a general phenomenon characteristic of sandwich dimers of aromatic molecules. The excited states are known as excimers, a word coined by Stevens and Hutton[10] to denote a dimer which is associated in its excited (emitting) state but which is dissociative (see Birks[11]) in its ground electronic state. The phenomenon was reported first by Foerster and Kasper[12] for the case of pyrene in solution.

Sandwich dimers are, in the simplest sense, the ground states of relaxed excimers. However, as the ground states are not very often stable their relationship to the excimer is not well defined in terms of inter- and intramolecular parameters. The large Stokes shift indicates a reduction of the interchromophore spacing in the excimer, but the emission contains no information about the effect of this reduction on other electronic states of the dimer.

Information about the electronic states of excimers can be obtained by measuring their transient absorption spectra, but there are significant limitations to the spectral range which can be probed and there are difficulties in obtaining information about polarization properties as well as the detection of weakly absorbing transitions.

An alternative approach, which circumvents the problems with the transient spectral method, involves the synthesis of bichromophoric compounds in which the two chromophores are linked by one or two chemical bridges. The latter case involves a new class of chemical compounds known as cyclophanes, the simplest and first to be synthesized being paracyclophane.[13] The relationship between the two chromophores in a cyclophane is, at all times, dominated by the constraints of the two connecting bridges. These constraints are partially lifted in the former case, that of one chemical bridge, and much can be learned from measurements with both types of coupled chromophores.

The absorption spectra of cyclophanes contain detailed information about the effects of interchromophore interactions on the energy levels of the separate chromophores, at intermolecular separations which are well below van der Waals distances. This information is augmented for the case of fluorescent cyclophanes, which have Stokes shifts much smaller than those observed for solution excimers. A major part of this article deals with the absorption spectra of cyclophanes for two reasons. Firstly, their spectra contain a wealth of information about the energy levels of sandwich dimers. Secondly, very often the spectra have been reported as just one of a group of physical properties which have been used to characterize new compounds, and there has been very little effort to compare and contrast the spectroscopic properties of different cyclophanes. This process is made more difficult because of the variation in the presentation of the data. Absorption spectra appear with either linear or logarithmic intensity ordinates while abscissae appear almost equally in units of wavelength or wavenumber. The published spectra were enlarged and then digitized in order to compare the various spectra in the literature. Once in this form it was a simple matter to use an efficient curve-handling routine to analyze the various data. The majority of the spectra reported here have been treated this way, so that authors might find it difficult to recognize their own data.

Sandwich dimers obtained by photocleavage of the photodimers of single bridged bichromophoric compounds provide data which are generally intermediate between those of the normal sandwich dimer and the corresponding cyclophane. The spectra of all three types of sandwich dimers therefore give us a very useful picture of the effect of an increasing interchromophore interaction on the energy levels of the dimer. As this article is primarily concerned with the electronic structures of sandwich dimers in their various forms, publications dealing with aspects of the luminescence of excimers or exciplexes are not included unless they provide some feature of the electronic structure of the excimer or exciplex which is relevant to this main theme.

Although the photocleavage of photodimers is an inherent part of the formation of sandwich dimers, the scope of this article is limited to the electronic spectroscopy of sandwich dimers and cyclophanes. Considerations of photochemistry are therefore omitted.

Finally a matter of terminology. A mixture of group theoretical representations and Platt's labels is used which might annoy some readers. The former is appropriate for cases of relatively high symmetry, especially those which have been the subject of theoretical treatments. However, for a variety of mixed cyclophanes, heterophanes, and low-symmetry cyclophanes these would be quite inappropriate, whereas the use of Platt nomenclature is quite clear.

II. Theory

A. Molecular Dimers

We consider a dimer consisting of molecules a and b and a dimer Hamiltonian H,

$$H = H_a + H_b + V_{ab}$$

H_a and H_b are the isolated molecule Hamiltonians and V_{ab} is the electrostatic interaction between the two molecules.

For each molecule we have a set of states i given by

$$H_a\Psi_a{}^i = E_a{}^i\Psi_a{}^i$$

$$H_b\Phi_b{}^i = E_b{}^i\Phi_b{}^i$$

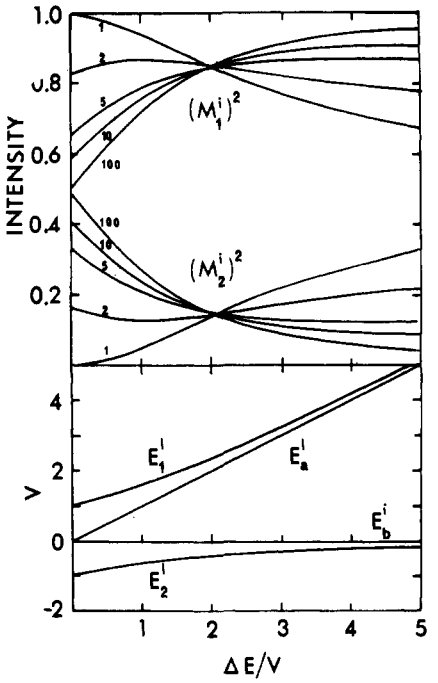

Figure 1. Lower panel: Energy levels of a dimer composed of different molecules ($E_{1,2}^i$). The monomer energy levels are given by E_a^i and E_b^i and the energies are in units of V. Upper panel: Normalized dimer intensities for various ratios $(\mathbf{M}_a^i)^2:(\mathbf{M}_b^i)^2$.

The ground-state ($i = 0$) wave functions for each molecule are

$$\Psi_a^0 = |\psi_1\bar{\psi}_1\cdots\psi_n\bar{\psi}_n| \quad (1)$$

$$\Phi_b^0 = |\phi_1\bar{\phi}_1\cdots\phi_m\bar{\phi}_m| \quad (2)$$

The ground state of the dimer is represented by a simple product wave function $\Psi_a^0\Phi_b^0$. The energy of the ground state of the dimer is

$$E^0 = \langle\Psi_a^0\Phi_b^0|H|\Psi_a^0\Phi_b^0\rangle$$
$$= E_a^0 + E_b^0 + V_{ab}^{00}$$

Before considering the excited states of the dimer we distinguish three possible cases.

(1) The molecules are identical and there is a symmetry operation which interchanges the two molecules.

(2) The molecules are identical but not related by symmetry.

(3) The molecules are not identical.

We have the following secular determinant to solve in each case

$$\begin{vmatrix} H^{i0,i0} - E & V^{0i,i0} \\ V^{i0,0i} & H^{0i,0i} - E \end{vmatrix} = 0$$

where

$$H^{i0,i0} = \langle\Psi_a^i\Phi_b^0|H|\Psi_a^i\Phi_b^0\rangle = E_a^i + E_b^0 + D_a^i$$

$$H^{0i,0i} = \langle\Psi_a^0\Phi_b^i|H|\Psi_a^0\Phi_b^i\rangle = E_a^0 + E_b^i + D_b^i$$

$$V^{i0,0i} = \langle\Psi_a^i\Phi_b^0|V_{ab}|\Psi_a^0\Phi_b^i\rangle = H^{i0,0i}$$

$$D_a^i = \langle\Psi_a^i\Phi_b^0|V_{ab}|\Psi_a^i\Phi_b^0\rangle$$

$$D_b^i = \langle\Psi_a^0\Phi_b^i|V_{ab}|\Psi_a^0\Phi_b^i\rangle$$

Case 1. For identical molecules the eigenfunctions are

$$\Omega_\pm^i = (\Psi_a^i\Phi_b^0 \pm \Psi_a^0\Phi_b^i)/\sqrt{2} \quad (3)$$

with eigenvalues

$$E_\pm^i = E^i + E^0 + D^i \pm V^{0i,i0}$$

The transition electric dipole moments are given by

$$\mathbf{M}_\pm^i = \{\mathbf{M}_a^i \pm \mathbf{M}_b^i\}/\sqrt{2}$$

Case 2. For identical molecules with no connecting symmetry operation we have

$$D_a^i \neq D_b^i$$

$$H^{i0,i0} \neq H^{0i,0i}$$

The eigenfunctions can be written as

$$\Omega_1^i = \cos(\gamma/2)\,\Psi_a^i\Phi_b^0 + \sin(\gamma/2)\,\Psi_a^0\Phi_b^i \quad (4)$$

$$\Omega_2^i = \sin(\gamma/2)\,\Psi_a^i\Phi_b^0 - \cos(\gamma/2)\,\Psi_a^0\Phi_b^i \quad (5)$$

where

$$\tan\gamma = 2V^{0i,i0}/(H^{i0,i0} - H^{0i,0i})$$
$$= 2V^{0i,i0}/\Delta D^i$$

and

$$\Delta D^i = D_b^i - D_a^i$$

The eigenvalues are

$$E_1^i = E^i + E^0 + D_a^i + \mathrm{V}\cot(\gamma/2)$$

$$E_2^i = E^i + E^0 + D_a^i - \mathrm{V}\tan(\gamma/2)$$

It can be seen that as $\Delta D^i \to 0$, $\gamma \to \pi/2$ and the eigenfunctions and eigenvalues approach those of case 1.

The transition electric dipole moments are

$$\mathbf{M}_1^i = \cos(\gamma/2)\,\mathbf{M}_a^i + \sin(\gamma/2)\,\mathbf{M}_b^i$$

$$\mathbf{M}_2^i = \sin(\gamma/2)\,\mathbf{M}_a^i - \cos(\gamma/2)\,\mathbf{M}_b^i$$

Case 3. In addition to the two inequalities of case 2 we have

$$E_a^i \neq E_b^i$$

If we write

$$\Delta E^i = E_b^i + E_a^0 - E_a^i - E_b^0$$

then the eigenfunctions have the same form as for case 2 but

$$\tan\gamma = 2V^{0i,i0}/(\Delta D^i + \Delta E^i) \quad (6)$$

and the eigenvalues are

$$E_1^i = E_a^i + E_b^0 + D_a^i + V^{0i,i0}\cot(\gamma/2)$$

$$E_2^i = E_a^i + E_b^0 + D_a^i - V^{0i,i0}\tan(\gamma/2)$$

In general we expect $\Delta E^i \gg \Delta D^i$, so we neglect ΔD^i.

The expressions for the electric dipole transition moments are the same as for case 2.

It is useful to see how the energy levels and absorption intensities of a dimer composed of two different molecules vary as a function of the parameter ΔE^i, in units of V. These variations are shown in Figure 1. As expected, the energy levels approach those of case 1 as the parameter approaches zero.

B. Configuration Interaction

The first-order dimer wave functions obtained above may be classified according to the representations of the point group of the dimer if it possesses symmetry. All those functions belonging to the same representation can mix. A convenient example is an anthracene

sandwich dimer in which the planes of each molecule are parallel, but the molecules have been rotated about their interplane axis. The point group symmetry of the dimer is then D_2 (case 1).

We consider the ^1L_a and ^1B_b states, polarized along the short (Y) and long (X) axes of each molecule, respectively. The monomer ^1L_a states give rise to dimer functions Ω_+^1 (Y polarization, B_2 representation) and Ω_-^1 (X, B_3) while the monomer ^1B_b states give dimer functions Ω_+^2 (X, B_3) and Ω_-^2 (Y, B_2).

Ω_+^1 and Ω_-^2 function will mix as will Ω_-^1 and Ω_+^2 functions. Configuration mixing of dimers was considered first by Craig[14] in his analysis of the absorption spectrum of crystalline anthracene. The effects are expected to be relatively minor if the interacting states are well separated. The main experimental effect will be a variation of polarization along the vibronic structure of each band system.

C. Intermolecular Excitation Exchange Integrals

A theoretical calculation of the dimer energy levels (including configuration interaction) requires evaluation of a number of intermolecular exchange integrals

$$V^{i0,0j} = \langle \Psi_a{}^1\Psi_b{}^0 | V_{ab} | \Psi_a{}^0\Psi_b{}^j \rangle$$

Two main methods of evaluation have been tried, (i) the so-called "dipole–dipole" approximation and (ii) a "distributed dipole–dipole" approximation.

If the intermolecular potential is expanded as a series of multipoles centered on each molecule the first nonvanishing term is

$$V^{i0,0j} = [\mathbf{M}_a{}^i \cdot \mathbf{M}_b{}^j - 3(\mathbf{M}_a{}^i \cdot r_{ab})(\mathbf{M}_b{}^j \cdot r_{ab})/r_{ab}{}^2]/r_{ab}{}^3$$

where the $\mathbf{M}$ are transition dipoles and r_{ab} is the vector connecting the two molecular centers. This is the familiar "dipole–dipole" approximation which has been used extensively in the calculation of the energy levels of molecular crystals,[15] dimers,[16,17] helical polymers,[18–20] and dye aggregates.[21] As the transition dipole moments can easily be obtained from experimental oscillator strengths, the method is very attractive. However, the multipole expansion is valid only if a sphere containing all the charge of one molecule does not overlap with a corresponding sphere for the other molecule.[22]

Craig and Thirunamachandran[23] examined the dipole–dipole approximation for molecular crystals and they concluded that sizeable errors will occur for anthracene because the distance between molecular centers is 5.237 Å. However, as the distance between molecular centers in a sandwich dimer may be as small as 3.5 Å, it is clear that very appreciable errors can be expected from this approach. Craig and Thirunamachandran[23] circumvented the problem for anthracene crystal by splitting the transition dipole moment into two parts, the central ring and the two outer rings, the division being made on the basis of the Hueckel MO (HMO) coefficients. At the same time Murrell and Tanaka[24] were investigating the anthracene excimer and in order to get around the breakdown of the dipole–dipole approximation they distributed the transition moment among the 14 carbon atoms, using the HMO coefficients.

As it is well known[24] that intensities calculated from the HMO coefficients are always too high by a factor of four or five, it is usual to scale the resultant exchange coupling energy by such an arbitrary factor or else use the experimental transition moment to scale the calculated value. However, in view of the extensive intensity losses which occur for the absorption spectra of the cyclophanes, compared with the intensities of the corresponding isolated chromophore spectra, even this procedure overestimates the excitation exchange integrals.

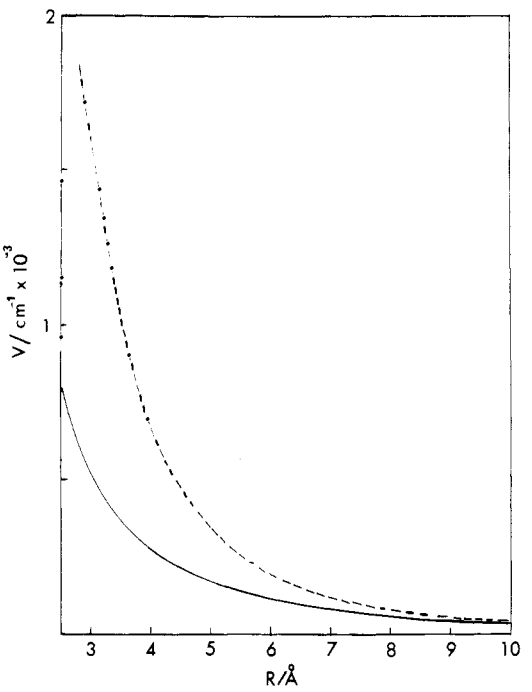

Figure 2. Values of the excitation exchange integral $V^{01,10}$ for a D_{2h} sandwich dimer as a function of interchromophore separation.[25] Values calculated using a distributed dipole method follow the full line while those calculated using a point dipole–dipole formulation are given by the broken line.

Morris[25] has compared the values of the excitation exchange integrals for the D_2 anthracene sandwich dimer (3.5-Å separation) calculated from the HMO coefficients and Pariser–Parr–Pople (PPP) SCF coefficients using the distributed dipole–dipole model. He found less than 4% difference in the two values. A comparison[25] between the distributed dipole–dipole method and the simple dipole–dipole approximation for the calculation of $V^{i0,0i}$ for the ^1L_a state of an anthracene sandwich dimer (D_{2h}) is given in Figure 2. Morris[25] has also calculated the excitation exchange integral for the ^1B_b state of anthracene for a 3.5-Å separation. He obtained a value of 2600 cm^{-1} using an experimentally scaled distributed transition moment compared with a value of 10 300 cm^{-1} for the dipole–dipole approximation.

D. Vibronic Coupling

So far the consideration of molecular dimers has neglected vibrational aspects, which complicate the understanding of their spectra. Each molecule has a characteristic absorption spectrum in which each electronic transition has a band structure composed of an electronic transition together with a number of vibrational side bands. The relative intensities of these features are determined by the relation between the excited state potential energy surface and that of the ground state. If the surfaces lie exactly over each other,

nearly all of the absorption intensity appears in a single band, the pure electronic origin. A displacement of the upper surface leads to intensity appearing in vibrational side bands, indicating the motion of the nuclei from their equilibrium ground state positions to new equilibrium positions in the excited electronic state.

In a molecular dimer the presence of an identical molecule leads to excitation transfer. If the rate of electronic excitation transfer is small compared with the time of a molecular vibration, we cannot separate the electronic and vibrational wave functions for the dimer and we write the dimer wave functions as

$$[\Psi_a{}^0\Psi_b{}^i\sigma_a{}^{00}\sigma_b{}^{ip} \pm \Psi_a{}^i\Psi_b{}^0\sigma_a{}^{ip}\sigma_b{}^{00}]/\sqrt{2}$$

where $\sigma_a{}^{ip}$ is the vibrational wave function of molecule a in the electronic state i and p is the vibrational quantum number. This is the weak coupling limit, considered first by Simpson and Peterson.[26]

If the rate of excitation transfer is fast compared to the vibrational time scale, then the dimer wave functions are

$$[\Psi_a{}^0\Psi_b{}^i \pm \Psi_a{}^i\Psi_b{}^0][\sigma_a{}^p\sigma_b{}^0 \pm \sigma_a{}^0\sigma_b{}^p]/2$$

This is the strong coupling limit.

The region between the weak and strong coupling limits, known as intermediate coupling, presents a very difficult problem which has been considered by numerous workers.[4,27-44] A most practical solution, in terms of computer analysis, is that due to Fulton and Gouterman (FG).[4] Their model uses two parameters, the excitation coupling parameter ($\epsilon = V^{0i,i0}$) and a displacement parameter (λ) which measures the displacement of the excited state surface along the coordinate of a single vibrational mode assumed to be involved in the vibronic transition.

Although the FG model lacks features present in real molecular dimers, such as anharmonicity and more than one active vibration, it provides a remarkable insight into the principal consequences of vibronic coupling. The most important of these is the intensity distribution in the dimer absorption spectrum. As the FG model belongs to case 1, the spectrum contains transitions to both in-phase and out-of-phase components of the dimer energy levels.

The intensity distributions of the two vibronic systems are markedly different in the weak and intermediate coupling regions when compared with the intensity distribution in the monomer spectrum. The lower energy system has an intensity distribution which falls more rapidly along the vibrational progression while the higher energy system has a distribution which rises and then falls along the progression. These intensity changes are usually recognizable even when ϵ is small, particularly if the orientation of the two molecules leads to unequal absorption intensities of the two dimer systems. These differences are illustrated by the absorption spectra of the anthracene sandwich and stable dimers (Figures 3 and 4).

Recent theoretical calculations of circular dichroism in the spectra of nonsandwich dimers, which incorporate vibronic coupling, require mention because of their consideration of the ^1L_b state of anthracene.[52,53] The authors concluded that the long-axis polarized absorption, lying under the predominately short-axis polarized absorption band in the near ultraviolet region, is better

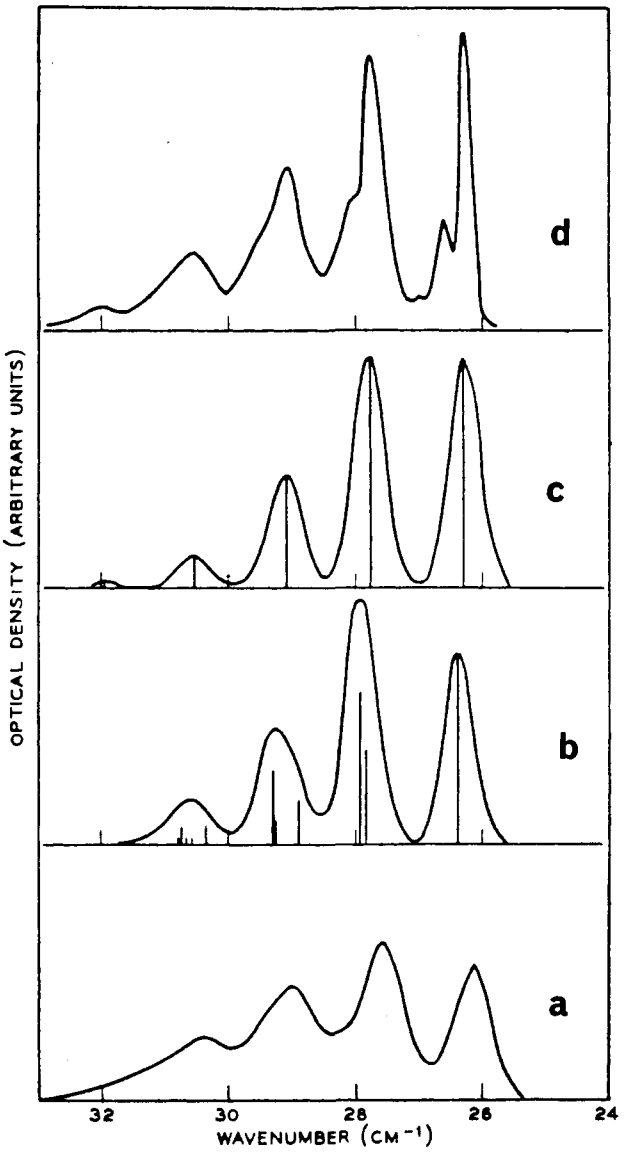

Figure 3. (a) Anthracene sandwich dimer at 77 K in methylcyclohexane.[3] (b) Computed dimer spectrum. (c) Computed monomer spectrum. (d) Monomer absorption spectrum at 77 K after softening rigid glass in (a). Gaussian profiles have been drawn in (b) and (c) with half widths of 350 cm^{-1}.

assigned to the ^1L_b state rather than a vibronically induced mixing of ^1L_a and ^1B_b states, as proposed by Michl et al.[54] The presence of the long-axis polarized absorption in the spectra of anthracenophanes is clearly seen and it is discussed in III.E.

E. Sandwich Dimers

A consequence of the different intensity distributions of the two systems is an unequal splitting of the electronic band of the monomer. As the lower energy component has a higher intensity (transition dipole), it is displaced more (to lower energy) than is the high energy component. This displacement is, however, far too small to explain the very large gap which is observed between the lowest energy absorption band of a sandwich dimer spectrum and the excimer fluorescence band arising from the sandwich dimer. It is necessary to consider another set of states, characteristic of the dimer, which are of the utmost importance for the energy levels of a sandwich dimer. These are the charge-transfer states, corresponding to transfer of electrons

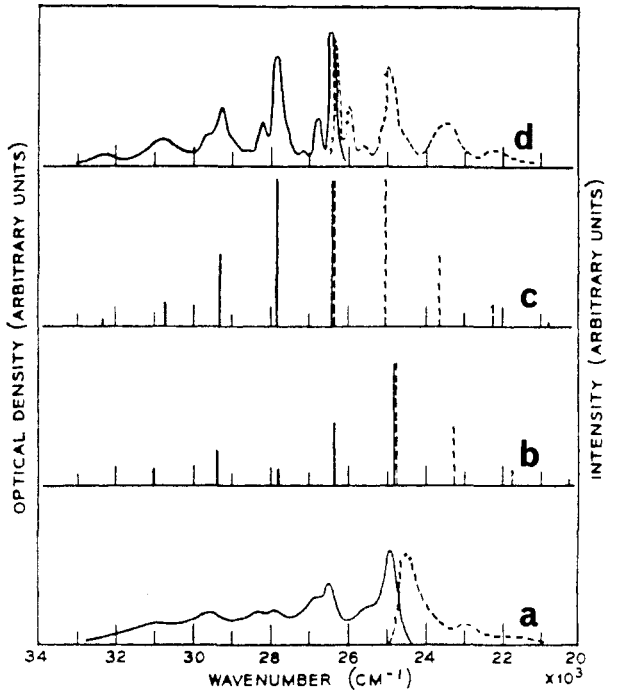

Figure 4. (a) and (b) show the observed and computed anthracene stable dimer absorption (full curves and lines) and fluorescence spectra, respectively.[3] (c) and (d) show the computed and observed anthracene monomer absorption (full curves and lines) and fluorescence spectra, respectively.

from one molecule to the other. Such states were considered first by Koutecky and Paldus[45-46] in their PPP treatment of paracyclophane. These states were also included in models for the excimer by Konijnenberg,[47] Murrell and Tanaka,[24] Azumi et al.,[48-50] and Vala et al.[51]

We illustrate the consequences of the inclusion of charge-transfer states for the case of anthracene. For each molecule the ground-state wave functions are given by (1) and (2) with $n = m = 7$. The first excited singlet state corresponds to the excitation of an electron from ψ_7 or ϕ_7 to ψ_8 or ϕ_8, respectively. The corresponding wave function can be written

$$\Psi_a{}^1 = \{|...\psi_7\bar{\psi}_8| - |...\bar{\psi}_7\psi_8|\}/\sqrt{2}$$

for molecule a and a similar one for molecule b. These are the locally excited states, and the dimer wave functions $\Omega_\pm{}^1$ are given by (3) of case 1 above. The analogous charge-transfer states arise from the excitation of one electron from Ψ_7 to Φ_8 or from Φ_7 to Ψ_8 and the corresponding charge-resonance states are given by

$$\Pi_\pm{}^1 = \{\Psi_a{}^{1+}\Phi_b{}^{1-} \pm \Psi_a{}^{1-}\Phi_b{}^{1+}\}/\sqrt{2}$$

To begin we assume that the dimer has the high symmetry of the perfectly overlapped geometry, i.e., D_{2h}. $\Omega_\pm{}^1$ then transform as B_{3g} (+) and B_{2u} (−) as do the analogous charge-resonance states. Corresponding sets of symmetry-related charge-transfer states exist for each of the locally excited states, e.g., both ^1L_b and ^1B_b each give rise to B_{3u} and B_{2g} locally excited and charge-transfer states of the sandwich dimer. Restricting consideration to the states arising from the ^1L_a monomer state the resulting states are

$$(a\Omega_+{}^1 \pm b\Pi_+{}^1)/\sqrt{(a^2 + b^2)}\ (B_{3g}{}^\pm)$$

and

$$(c\Omega_-{}^1 \pm d\Pi_-{}^1)/\sqrt{(c^2 + d^2)}\ (B_{2u}{}^\pm)$$

Azumi, Armstrong, and McGlynn[49] as well as Murrell and Tanaka[24] have given the calculated energies of these states as a function of intermolecular separation for anthracene, and both sets of workers concluded that the lowest excited state is the $B_{3g}{}^-$ state.

Exactly analogous consideration can be given to the various states arising from the molecular ^1L_b and ^1B_b states, both of which are polarized along the long axis of the molecule. In this case the dimer states belong to the representations $B_{2g}{}^\pm$ and $B_{3u}{}^\pm$, and there can be configuration interaction mixing between those states which belong to the same representation.

Azumi and McGlynn[50] have given a group theoretical analysis of charge resonance and excitation resonance states of sandwich dimers with D_{6h} and D_{2h} symmetry as well as dimers of lower symmetry. Two of these are relevant for the sandwich dimer of anthracene in relation to the two conformers of [2.2](9,10)-anthracenophane. These conformers have symmetry C_{2h} (translated conformer) and D_2 (rotated conformer) and are considered in IV.E. It should be noted, however, that Azumi and McGlynn[50] have discussed the rotated conformer under the point group C_2 instead of D_2, so their conclusions are in error for this conformer.

The essence of these approaches to the calculation of the energy levels of the sandwich dimer is one of configuration interaction between dimer states derived from localized and charge-transfer states. The alternative approach is to treat the sandwich dimer as a single molecule and carry out a molecular orbital calculation to find the energy levels. This latter method was used by Koutecky and Paldus (KP)[45-46] for paracyclophane while Vala et al. (VHRJ)[51] used the configuration interaction approach for the same molecule. A comparison of the two methods for paracyclophanes is given in III.A.

III. Cyclophanes

A. Paracyclophanes

A systematic study of the absorption spectra of a number of paracyclophanes ([*m.n*]PC) was undertaken by Cram et al.[55] in order to see the effects of variations in the lengths of the methylene bridges. Cram and Steinberg[56] had earlier observed marked differences in the absorption spectra of [2.2]PC, [2.3]PC, and [2.4]PC, so the work of Cram et al.[55] was designed to find the reasons for the spectral changes. These were assumed to be either π-electron interactions between the rings or loss of planarity of the rings.

Cram et al.[55] found only subtle changes in the absorption spectra of [5.6]PC, [5.5]PC, [4.5]PC, and [4.4]PC. However, they observed marked changes for the absorption spectra of [3.4]PC, [3.3]PC, [2.3]PC, and [2.2]PC. They assessed their observations in relation to the idealized calculated molecular geometries of the various paracyclophanes. On this basis the calculated separation for [3.4]PC was given as 2.84 Å (closer end) while for [4.4]PC the separation between the two planes was calculated as 3.73 Å.

Cram et al.[55] also studied the absorption spectra of analogous compounds in which one benzene ring was either reduced to cyclohexane or replaced by methylene

groups. These measurements were made to assess the effects of warping of the aromatic ring in the strained molecules. They concluded that part of the spectral changes observed in the spectra of the paracyclophanes is due to the loss of planarity of the benzene rings.

The work of Cram et al.[55] pointed, fairly clearly, to π-electron interactions and the loss of ring planarity, both of which become important if the separation between facing aromatic rings becomes less than 3.40 Å, as being the cause of the observed spectral changes. The term transannular interaction is commonly used to cover both of these effects. The rather extensive absorption data of Cram et al.[55] warrant much closer inspection than is possible from the data as presented in their paper. Their spectra are considered in more detail below, after first examining the various theoretical calculations relevant to the paracyclophanes.

The first attempt at spectroscopic analysis was made by McClure[57] who applied a simple coupled chromophore model to the lowest energy bands. This was based on the splitting of the degenerate benzene chromophore energy levels, by excitation resonance, into in-phase and out-of-phase components ($\Omega_{\pm}^{1}$, (3) II.A.). McClure[57] used a dipole–dipole approximation to estimate the resonance splitting of the two lowest dimer states, but this fell far short of the assigned splitting for [2.2]PC. Ingraham[58,59] used valence–bond and simple Hueckel MO LCAO methods to consider the effect of transannular interactions on the energy levels of [2.2]PC but not in a detailed way. The first detailed theoretical examination of these systems was provided by KP[45,46] who used a semiempirical SCF LCAO MO approach. They used a high-symmetry, undistorted geometry for the dimer with D_{6h} symmetry. Within this framework electronic transitions from the ground state fell into two classes, excitations within one benzene ring and electron transfers from one ring to the other. We use Platt's nomenclature for single molecule states and point group representations to denote dimer states. The calculations showed a strong asymmetrical splitting of each degenerate pair of states arising from the ^1L_b ($^1B_{2u}$ and $^1B_{1g}$ in the dimer), the ^1L_a ($^1B_{1u}$ and $^1B_{2g}$ in the dimer), and the ^1B (^1E_u and ^1E_g in the dimer) states of the benzene chromophore with decreasing ring separation. KP[46] made spectral assignments for [4.4]PC, [3.3]PC, and [2.2]PC by using the data of Cram et al.,[55] which are discussed further below.

VHRJ[51] adopted a different approach, analogous to the theoretical models developed by Konijnenberg,[47] Murrell and Tanaka,[24] and Azumi et al.[48-50] for the understanding of excimers of polycondensed aromatic hydrocarbons. This involved a calculation of configuration interaction between a set of dimer excitation resonance states and a set of dimer charge resonance states, as a function of the intermolecular separation.

As well as using the data of Cram et al.,[55] VHRJ[51] were able to interact with Ron and Schnepp,[60,61] who had measured the absorption and fluorescence spectra of single crystals of [2.2]PC. The crystal structure had been determined by Brown[62] and Lonsdale et al.,[63] so that Ron and Schnepp were able to determine the polarization of the lowest energy absorption band as well as that of the fluorescence.[61] They found that at 20 K there was a common origin for both absorption and fluorescence in the form of a weak line at 30 361 cm^{-1}, polarized parallel to the long axis of the molecule. They also observed another weak origin at 30 741 cm^{-1} in the absorption spectrum, which was polarized parallel to the short molecular axis.

The theoretical calculations of VHRJ,[51] based on a centrosymmetric dimer of high symmetry (D_{6h}), the same as assumed by KP,[46] gave the dimer state $^1B_{1g}$ as the lowest excited state for all ring separations (as does the KP model). This assignment was in apparent variance with the data of Ron and Schnepp[61] because electronic transitions to and from the ground state are forbidden. Ron and Schnepp[61] postulated a torsional distortion of one ring relative to the other, about the interchromophore axis, in the excited state, thereby providing a weakly allowed character to the transition to and from this state.

The D_{6h} dimer calculations by VHRJ[51] gave the next excited state about 3000 cm^{-1} higher in energy. This is the other component ($^1B_{2u}$) of the monomer ^1L_b state, and the allowed electronic transition should be polarized parallel to the short molecular axis. However, because of its weakness this origin was assigned to the $^1B_{2g}$ component of the dimer pair arising from the monomer ^1L_a state. Calculations using more realistic nonplanar rings in the dimer showed that this state should be depressed below the $^1B_{2u}$ state.

A reinvestigation of the crystal structure of [2.2]PC by Hope et al.[64] showed that the molecule actually has D_2 symmetry and the structure is disordered with respect to the orientation of the molecule in its site. The adoption of this conformation allows the atom–atom repulsion energies, inherent in the fully eclipsed conformation, to be relieved. Another possible conformation involves a translation of one chromophore relative to the other along the long molecular axis. However, molecular mechanics calculations show that this conformation does not provide a true minimum and, unlike the [2.2]anthracenophanes for example, [2.2]PC appears to have only one stable conformation.

The theoretical calculations of VHRJ[51] and those of KP[46] are compared in Figure 5. They differ in their order of states, particularly at separations of less than 3.5 Å. The interaction between the localized and charge resonance states connected with the ^1B single molecule state is stronger for the KP calculations because the states are nearly degenerate at larger separations.

An important difference between VHRJ and KP lies in the magnitudes of the splittings of each pair of dimer states, which correlate with the monomer states, i.e., the solid lines in Figure 5. For a 3-Å separation the splittings are 3000, 1000, and 8500 cm^{-1} for VHRJ and 6000, 9500, and 17 000 cm^{-1} for KP, in order of increasing energy of the parent monomer states. The next significant difference is the independence of the u-dimer-state energies on ring separation for KP, in contrast to those for VHRJ.

It is instructive to examine the data of Cram et al.[55] in relation to the calculations of VHRJ and KP. Their spectral data were digitized and the data for [4.4]PC, [3.3]PC, [3.2]PC, [2.2]PC, and a model compound (1,4-bis(n-pentyl)benzene) are displayed in Figures 6 and 7 together with the integrated absorption intensities (oscillator strengths).

Turning to Figure 7 we see that the oscillator strength of [2.2]PC is the largest across the whole of the spectral

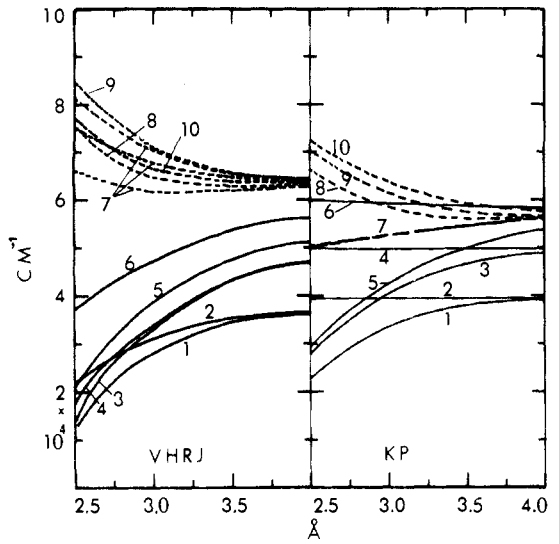

Figure 5. Theoretical energy levels for paracyclophane as a function of intermolecular separation for the D_{6h} dimer. States: 1 (B_{1g}), 2 (B_{2u}), 3 (B_{2g}), 4 (B_{1u}), 5 (E_{1g}), 6 (E_{1u}), 7 (B_{2u}, B_{1u}, E_{1u}), 8 (B_{1g}), 9 (B_{2g}), 10 (E_{1g}). The left hand panel shows the calculations of Vala et al.[51] and the right hand panel those of Paldus and Koutecky.[46] The broken curves correspond to the charge resonance states.

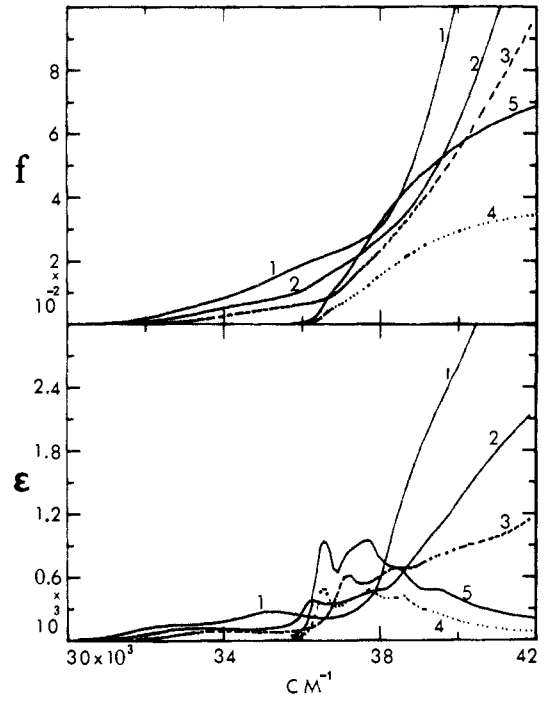

Figure 6. Lower panel: Room-temperature solution molar absorption spectra of the following paracyclophanes,[55] [2.2]PC (1), [3.2]PC (2), [3.3]PC (3), and [4.4]PC (4). The spectrum of the model compound 1,4-di-*n*-pentylbenzene is given (5). Upper panel: Corresponding oscillator strengths (f).

region. At 48000 cm^{-1} the model compound has the next largest oscillator strength while [3.3]PC has the smallest value. It seems that for [3.2]PC, [3.3]PC, and [4.4]PC there is an overall shift of intensity out of the region below 48000 cm^{-1} into the region at higher energy. The same movement is also observed in the spectra of [4.3]PC, [2.4]PC, [3.6]PC, and [4.6]PC, and it is only for [2.2]PC that the reverse holds. From Figure 6 we see that between 30000 and 42000 cm^{-1} it is only [4.4]PC which has a lower oscillator strength than the open compound, the other compounds having

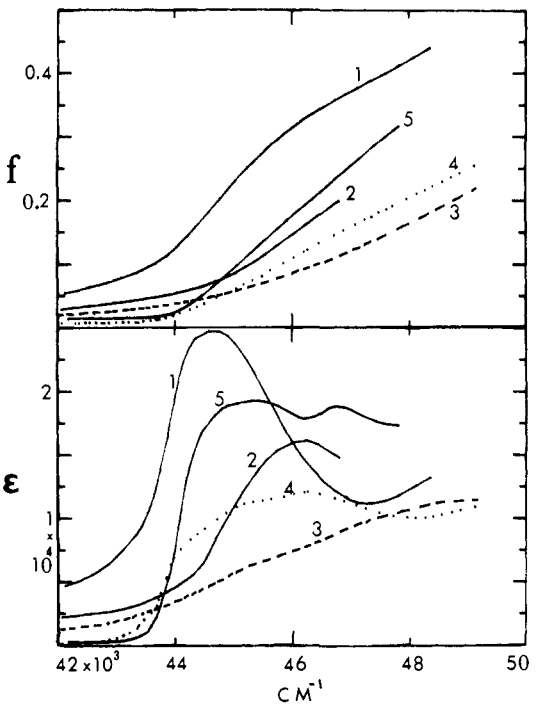

Figure 7. Same as for Figure 6.

larger absorption intensities. The effect of transannular interaction at larger interchromophore separations is to remove absorption intensity from the ^1L_a band and, presumably, shift it to higher energy. On the other hand there is movement of intensity into the region between 30000 and 42000 cm^{-1} for all but [4.4]PC. The latter statement is also true for [4.6]PC, but not for [3.6]PC.

The data in Figures 6 and 7 suggest that at larger separations, equivalent to that for $n = m = 4$, absorption intensity is lost from the ^1L_b band while the ^1L_a band moves to higher energy. As well as an overall intensity loss for all transitions, as occurs for the anthracenophanes (III.G.), there are two possible reasons for these intensity changes. One involves the charge resonance states which lie at higher energy (see Figure 5 for theoretical predictions). As the interchromophore separation is reduced, their interaction with the localized states becomes more important. The intensity of a localized transition is then shared with the associated charge resonance transition, so that this process will move intensity out of the region under discussion. A second reason is simply that the allowed component of the dimer state arising from ^1L_a moves to higher energy with decreasing chromophore separation, before moving to lower energy because of increasing destabilization of the ground state. This behavior is inconsistent with the VHRJ model and suggests that the in-phase component derived from the ^1L_a state (which will carry more of the intensity) is shifted to higher energy. At smaller separations the distortions forced on the chromophores allow the forbidden out-of-phase dimer component derived from the ^1L_a monomer state to provide intensity in the region of the ^1L_b monomer band, and this can explain the observed intensity increase in the region of 38000–42000 cm^{-1}. For the case of [2.2]PC there is a net increase of intensity across the whole of the spectral region, below 48000 cm^{-1} and it is likely that the effect of out-of-phase intensity from the intense ^1B transition of the monomer in the vacuum ultraviolet region is

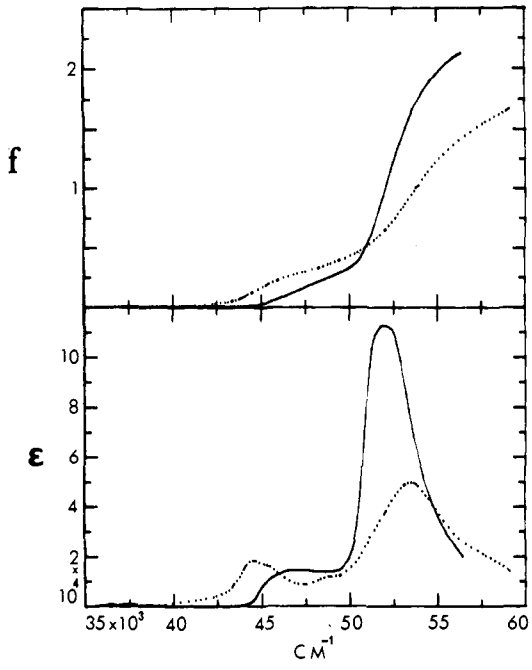

Figure 8. Lower panel: Room-temperature solution molar absorption spectra of *p*-xylene (full curve) and paracyclophane.[65] Upper panel: Corresponding oscillator strengths (f).

responsible for this increase.

This analysis suggests that the splitting of the ^1L_a state-derived dimer state is considerably larger than the VHRJ calculations provide and more in line with those of KP. In addition, for [2.2]PC, it seems clear that it is necessary to invoke the out-of-phase components of the ^1B derived states in the region below 48 000 cm^{-1} to explain the high intensity of the [2.2]PC absorption spectrum. Of course these conclusions are phenomenological and they are, as yet, not supported by polarization data, apart from that provided by Ron and Schnepp.[60,61]

There are inherent difficulties in understanding the effects of transannular interactions on the energy levels of the benzene chromophore on the basis of a partial observation of the overall electronic transitions. Iwata et al.[65] have helped to remedy this through their very important measurement of the vacuum ultraviolet spectrum of [2.2]PC in hydrocarbon solution (up to 59 000 cm^{-1}) as well as single crystal measurements covering the range of 30 000–50 000 cm^{-1}. Their solution spectrum is shown in Figure 8 together with the absorption spectrum of *p*-xylene, both in the lower panel, while the integrated absorption intensities are given in the upper panel. These data make it clear that the band at 45 000 cm^{-1} is essentially the in-phase dimer component derived from ^1L_a and the intense band at 53 000 cm^{-1} corresponds to the in-phase dimer components derived from ^1B. However, it is also clear that there is additional intensity in the region below 48 000 cm^{-1}, which must come from states derived from ^1B.

Fuke and Nagakura[66] extended the single-crystal polarization information through measurements of polarized reflectivity from a (011) face in the region of 20 000–60 000 cm^{-1}. By means of a Kramers–Kroenig transformation they obtained polarized absorption spectra which reveal the anisotropy of the absorption to 60 000 cm^{-1}, shown in Figure 9. The projections of the molecules on the (011) face are included in Figure

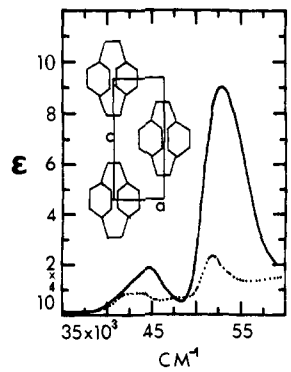

Figure 9. Single-crystal absorption spectrum of paracyclophane for light normal to the (011) face[66] at room temperature. The full curve is for light polarized parallel to *c*, and the broken curve is for light polarized parallel to *a*. The inset shows the projections of the molecules on the (011) face.[62–64]

9, and it can be seen that the two sets of spectra discriminate between the two in-plane polarization directions of each *p*-xylene chromophore. This discrimination is not exact because the molecule has the rotated D_2 conformation, which lacks a centre of symmetry. The band near 45 000 cm^{-1} in solution (Figure 8) is seen from the crystal polarization to have intensity $\|a$ as well as the expected intensity $\|c$ so the band cannot be purely the in-phase component derived from ^1L_a monomer state as concluded in the previous paragraph. Fuke and Nagakura[66] assigned the *a* polarized intensity to one component of an in-phase E_u-charge-transfer state which mixes strongly with the locally excited E_u state. The other component will have *c* polarized intensity, so the band at 45 000 cm^{-1} was therefore assigned to transitions to the two charge-transfer states and the in-phase component derived from the monomer ^1L_a state. An alternative assignment would have the two out-of-phase components of the states derived from the monomer ^1B state responsible for the additional absorption intensity in this spectral region. Fuke and Nagakura[66] have, instead, assigned these latter transitions to the band at 35 000 cm^{-1} (Figure 8). The analysis of the data of Cram et al.,[55] given above, tends to favor an assignment of the band at 35 000 cm^{-1} to the in-phase component of the state derived from ^1L_b and the out-of-phase component of the state derived from ^1L_a. Fuke and Nagakura[66] assigned the former to the broad shoulder near 39 000 cm^{-1} (Figure 8), but this assignment is not consistent with the conclusions reached from a comparison of the various paracyclophane spectra of Cram et al.[55] The analysis of Fuke and Nagakura[66] was based on the crystal structure deterinations of Brown[62] and Lonsdale et al.[63] by use of a D_{2h} symmetry for the dimer for which the out-of-phase components would have zero intensity. Fuke et al.[67] have reported some two photon measurements of [2.2]PC, which they used to support the assignments of Fuke and Nagakura.[66]

A disturbing feature of the spectrum in Figure 9 is the very small intensity of the *a* polarized absorption above 50 000 cm^{-1} compared with the much stronger *c* polarized absorption intensity. Orientation factors lead to a loss of one half of the short-axis-polarized intensity in the *a* polarization, but this still leaves a very big discrepancy as the chromophore absorption intensity should be polarized equally along the short and long chromophore axes.

The overall features of the absorption spectra of the paracyclophanes are seen to be closer to the calculations of KP than those of VHRJ. The important discrepancy between the experiment and theory, so far as the VHRJ calculations are concerned, is the observed large splitting of the ^1L_a state in the paracyclophanes. Even at larger separations the evidence favors an upward movement of the in-phase component while a significant downward movement of the out-of-phase component is also evident. This result conflicts with the VHRJ calculations (see Figure 5). Certainly, the assignments made by VHRJ cannot be sustained, except for the states derived from the $^1B_{2u}$ monomer state. The assignments suggested by KP[46] come much closer to those arrived at by the present analysis. Iwata et al.[65] have also carried out theoretical calculations using the method of VHRJ, and they pointed to problems in the assignments made by VHRJ. In their model the effect of configuration interaction between locally excited and charge-transfer configurations leads to a larger splitting of the states derived from ^1L_a, but the in-phase component still lies appreciably below the monomer position. Also, the intense band associated with the E_u in-phase allowed components is observed well below the calculated position.

The calculations by KP[46] and VHRJ[51] are based on $\sigma-\pi$ separability and Gleiter[68] pointed out that the two π systems can interact via the σ bonds of the methylene bridges, and it would be dangerous to neglect these. He suggested that the splitting of the lowest energy dimer pair state could be significantly reduced by inclusion of "through bond" interactions. Hoffmann[69] has developed the concepts of "through space" and "through bond" interactions, and Heilbronner and Yang[70] have reviewed the interpretation of paracyclophane photoelectron spectra within this framework. Their analysis points rather clearly to the importance of both types of interaction in determining the overall orbital energy patterns in paracyclophanes. It remains for "through bond" interactions to be included in new treatments of the excited states of paracyclophanes.

There has been very little research into the luminescence spectra of the paracyclophanes. The work of Ron and Schnepp[61] on [2.2]PC has been mentioned above. Matsui et al.[71] reported observations of delayed fluorescence from crystals and rigid glass solutions at 4.2 K. They suggested the formation of a biradical species involving cleavage of one of the bridges. Recombination of this species to re-form [2.2]PC in its excited electronic state is then responsible for the delayed fluorescence. Vala et al.[72] reported the fluorescence of [4.4]PC, [4.5]PC, and [6.6]PC at room temperature. Anomalous (excimer) emission was only found for [4.4]PC. More recently Otsubo et al.[73] prepared [3.3]PC and [4.4]PC, and they reported excimer emission from the former at room temperature and at 77 K, but only excimer emission from [4.4]PC at room temperature. At 77 K they found monomer emission, and they concluded that at 77 K the molecules are not in the correct conformational relationship to allow the formation of the excimer.

B. Metacyclophanes

[2.2]Metacyclophane was prepared first in 1899[74] and its molecular structure was determined by X-ray diffraction.[75] The molecule adopts a chair (anti) conformation with no overlap of the π electrons from different rings. Sato et al.,[76] from a NMR study, concluded that over the temperature range from −80 to 190 °C the molecule is frozen in the chair conformation. The barrier to ring inversion was estimated by Griffin et al.[77] to be 26–28 kcal/mol. Allinger et al.[78] examined its physical properties including the ultraviolet absorption spectrum. The spectrum was compared to that of a control compound in which one of the benzene rings was saturated, and the spectral differences were ascribed to ring warping.

Shizuka et al.[79] reported both monomer and excimer fluorescence from [2.2]metacyclophane in cyclohexane solution at room temperature with quantum yields of 2×10^{-5} and 5×10^{-6}, respectively. They postulated an excited-state conformational change from anti to syn form to explain the excimer. They were unable to detect phosphorescence at 77 K. These results appear to be at variance with later observations by Otsubo et al.,[80] who reported only excimer emission (different wavelength maximum) at room temperature and only monomer fluorescence and phosphorescence at 77 K.

Otsubo et al.[80] have also studied the spectral properties of [3.3]metacyclophane. The absorption spectrum is very broad and significantly different from that of [2.2]metacyclophane. The differences were ascribed to conformational flipping between syn and anti forms but no temperature dependent studies, which might help substantiate this explanation, were given. They reported both monomer and excimer fluorescence at room temperature but only monomer emission at 77 K.

C. Metaparacyclophanes

The ultraviolet absorption spectrum of [2.2]metaparacyclophane was reported by Hefelinger and Cram.[81] More recently Otsubo et al.[80] have examined the spectral properties of [2.2]metaparacyclophane and [3.3]-metaparacyclophane. They reported weak transannular interaction for the former and none for the latter. They also reported that both compounds show monomer and excimer fluorescence at room temperature but only monomer fluorescence at 77 K.

D. Naphthalenophanes

Two naphthalene chromophores can be coupled together in a large number of ways and there has been considerable interest in the photoelectron spectra of these compounds.[70]

The first optical study[82] involved [2.2](1,4)-naphthalenophane ([2.2](1,4)NN) in its two isomeric (syn and anti) forms, and the room-temperature absorption and fluorescence spectra were given along with the phosphorescence spectra. Recently Yoshinaga et al.[83] have reported the absorption spectra of syn and anti forms of [3.3](1,4)naphthalenophane, and they found fluorescence maxima at 430 nm (syn isomer) and 420 nm (anti isomer). They also gave the absorption spectra of the two [2.2](1,4)naphthalenophanes.

More recently Blank and Haenel[84] have prepared the syn and anti isomers of [2.3](1,4)naphthalenophane, and they have given the room-temperature absorption spectra. It is extremely interesting to compare the absorption spectra of each of these isomers with the

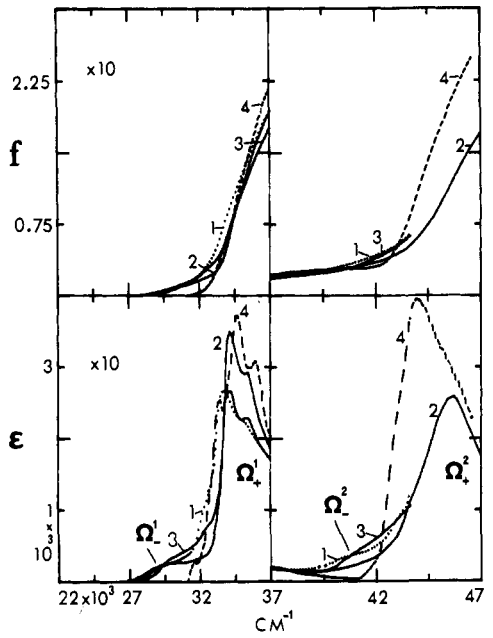

Figure 10. Lower panels: Room-temperature solution molar absorption spectra of *s*[2.2](1,4)NN[83] (1), *s*[2.3](1,4)NN[84] (2), *s*[3.3](1,4)NN[83] (3) and DMN (4; 2 × ε). Upper panels: Corresponding oscillator strengths (f).

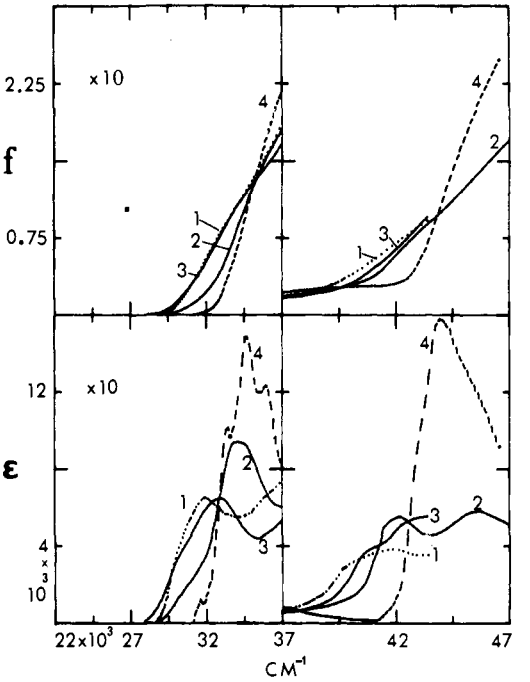

Figure 11. Lower panels: Room temperature solution molar absorption spectra of *a*[2.2](1,4)NN[83] (1), *a*[2.3](1,4)NN[84] (2), *a*[3.3](1,4)NN[83] 93) and DMN (4; 2 × ε). Upper panels: Corresponding oscillator strengths (f).

spectra of the corresponding isomers of the [2.2](1,4)- and [3.3](1,4)naphthalenophanes with the spectrum of 1,4-dimethylnaphthalene as a reference spectrum. The spectra are shown in Figures 10 and 11.

Even though the spectra of Yoshinaga et al.[83] do not extend to as a high a wavenumber as the other spectra, so that the effects of interchromophore interaction are not completely clear, the comparisons provide an impressive qualitative insight into the effects of transannular interactions in the two types of isomer. As a first approach we use the simple coupled chromophore model, II.A. case 1.

There is no doubt that the syn isomers provide a greater overlap of the two π-electron systems than the anti isomers do, but the spectral effects appear to be much less marked for the syn isomers, and the qualitative features appear to be the following. The intense ^1B_b band appears to split into two components with the in-phase (dipole allowed Ω_+^2) component shifted to higher energy by about 2000 cm^{-1}, and the lower (out-of-phase Ω_-^2) component shifted to lower energy by a little more. The latter state is seen as a weak transition between 40 000 and 42 000 cm^{-1} (Figure 10).

The medium intense ^1L_a band has its in-phase Ω_+^1 component shifted slightly to lower energy in each of the three cyclophanes, and there is a band in all three spectra between 27 000 cm^{-1} and 31 000 cm^{-1} which could be the out-of-phase dimer Ω_-^1 component of the ^1L_a state. This is as far as can be gone with these room-temperature solution spectra, and low-temperature data are required before more detailed interpretations can be reached.

Whereas the syn isomer spectra appear to be straightforward in their interpretation, the absorption spectra of the corresponding anti isomers are, oddly, much more complex, even though the orbital overlap between the two chromophores must be considerably less than for the syn isomers. It appears from the spectra that the ^1B_b monomer band is split into two, roughly equally intense, bands. This conclusion is supported by the integrated absorption intensities (oscillator strengths) of both sets of isomers as well as that for 1,4-dimethylnaphthalene shown in Figure 11. Even though the data for the [2.2] and [3.3] cyclophanes do not extend beyond 43 000 cm^{-1}, it appears reasonably clear that the overall oscillator strength of the parent chromophore is conserved in the three cyclophane spectra, in spite of considerable spectral distribution changes.

We note also, from Figure 11, that the changes in the ^1L_a band are unusual. This band moves to low energy, apparently, but there is a considerable loss of intensity. The lost intensity reappears in the region above 35 000 cm^{-1} where it merges with a lower energy component derived from the ^1B_b band. It seems that, like the ^1B_b band, the ^1L_a band also splits into two bands of roughly equal intensity. Neither behavior can be understood on the basis of the simple coupled chromophore approach. The approximate symmetry of the anti isomers is C_{2h}, and the out-of-phase components ($\Omega_-^{1,2}$) arising out of the coupling between the chromophores should have zero or near zero intensity, in distinct contrast to the observed behavior. Clearly, these compounds require much more detailed spectroscopic examination than has presently been given. However, consideration of charge resonance states allows a qualitative analysis of the observed behavior, similar to that found for the anthracenophanes (III.E.3.). For each dimer state derived from a given monomer state there is an analogous charge resonance state. The interaction between corresponding localized and charge resonance states will vary with the amount of overlap between the two chromophores. If the two sets of states are nearly equally mixed for the symmetrical conformation, the intensity of the transition to the out-of-phase component will be very small because of the cancellation of the component moments (syn isomer). For the anti

isomer the overlap is significantly less and the intensities no longer cancel, so both absorption transitions carry intensity (see III.E.3.).

E. Anthracenophanes

1. Introduction

The anthracenophanes have attracted, by far, the most serious spectroscopic effort among the cyclophanes. All of the absorption bands of interest are in an easily accessible spectral region so no special techniques are required. The photochemical reactivity of anthracene has also been a motivation for the study of many of the various anthracenophanes which have been prepared. The connecting bridges have so far been confined to the (9,10) and (1,4) positions.

2. [2.2]Anthracenophanes

The first anthracenophane to be described was [2.2](9,10)anthracenophane ([2.2](9,10)AA). This was prepared by Golden,[85] who also noted the presence of two distinct crystal modifications (α and β) and the facile photochemical transformation of [2.2](9,10)AA into its colorless photoisomer dianthracene.

Three other [2.2] anthracenophanes were then prepared by Umemoto et al.[86] and by Iwama et al.,[87] and their room-temperature absorption spectra were reported. These compounds are [2.2](1,4)(9,10)-anthracenophane ([2.2](1,4)(9,10)AA), *syn*-[2.2](1,4)-anthracenophane (*s*[2.2](1,4)AA), and *anti*-[2.2](1,4)-anthracenophane (*a*[2.2](1,4)AA).

A more complete characterization of these three new anthracenophanes was given by Iwama et al.[88] *s*-[2.2](1,4)AA was shown to form a photoisomer which regenerated the other isomer by ultraviolet irradiation and by heat. Both isomers were characterized by X-ray structure determination, and NMR data were given for all three compounds. Room-temperature solution absorption spectra were again reported, but no detailed analysis of the spectra was given.

Whereas [2.2](9,10)AA is nonfluorescent, the other three [2.2]anthracenophanes all show fluorescence, and details of their excimer spectral properties were reported by Hayahsi et al.[89] As might be expected from their molecular structures, the molecule with the largest overlap of the rings, *s*[2.2](1,4)AA, has its fluorescence at lowest energy, while that with the least overlap of the rings, *a*[2.2](1,4)AA, has its fluorescence at highest energy. The latter emission also shows signs of structure in its room-temperature spectrum, in contrast to the broad excimer emission bands from the other two anthracenophanes. This work reinforced previous conclusions[90-92] that an excimer emission band is not a characteristic and unique property of a sandwich dimer, but rather there are different excimer emission profiles from a given sandwich dimer, dependent on variations of the orientational overlap for that dimer.

The four [2.2] anthracenophanes provide a variety of chemical sandwich dimer geometries for two anthracene chromophores and their different spectral and photochemical properties represent a challenge for theoretical investigation and interpretation. Their absorption and fluorescence spectra were then reexamined by Morita et al.[93] and theoretical calculations carried out, using the excitation resonance and charge resonance configuration model, with PPP SCF MO's.

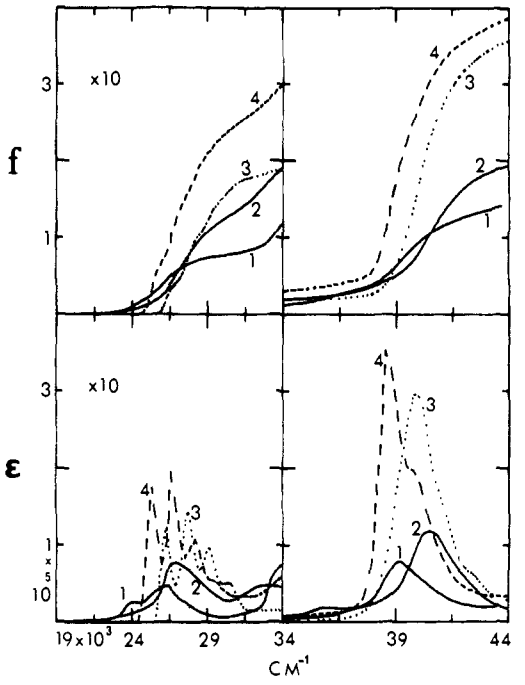

Figure 12. Lower panels: Room temperature solution molar absorption spectra[93] of [2.2](9,10)AA (1), *s*[2.2](1,4)AA (2), (1,4)DMA (3; 2 × ϵ) and (9,10)DMA (4; 2 × ϵ). Upper panels: Corresponding oscillator strengths (f).

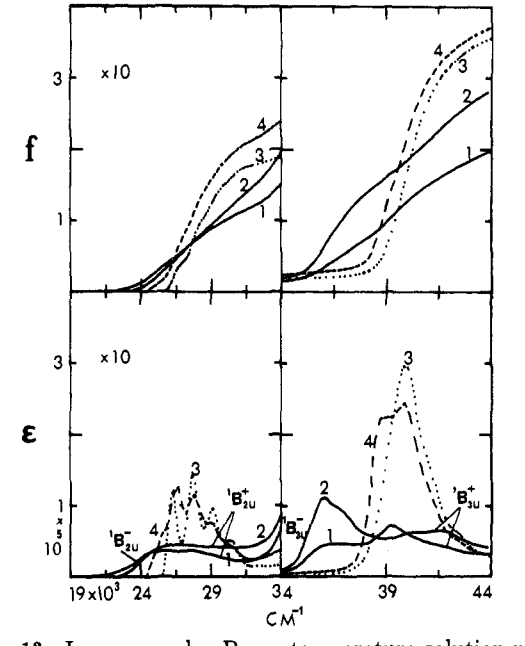

Figure 13. Lower panels: Room-temperature solution molar absorption spectra[93] of [2.2](1,4)(9,10)AA (1), *a*[2.2](1,4)AA (2), (1,4)DMA (3; 2 × ϵ) and (1,4)DMA + (9,10)DMA (4). Upper panels: Corresponding oscillator strengths (f).

Before considering details of the analysis of the anthracenophane spectra, it is of considerable benefit to examine the overall spectral features of the four compounds, particularly in relation to the absorption spectra of 1,4-dimethylanthracene (DMA) and 9,10-dimethylanthracene ((9,10)DMA). It is most convenient to separate this examination into the two pairs [2.2]-(9,10)AA with *s*[2.2](1,4)AA and *a*[2.2](1,4)AA with [2.2](1,4)(9,10)AA. The room-temperature spectra are shown in Figures 12 and 13, along with the integrated

absorption intensities, expressed as oscillator strengths. There are many points to consider from these data.

We note from Figures 12 and 13 that the spectra of *s*[2.2](1,4)AA and [2.2](9,10)AA show some resemblance as do those of the other pair, but there is no significant cross resemblance. Also, we see that the integrated absorption intensities (to 44 000 cm^{-1}) show a pronounced loss of oscillator strength compared with the spectra of the parent chromophores. This loss is greatest for [2.2](9,10)AA (largest overlap) and least for *a*[2.2](1,4)AA (least overlap).

These simple comparisons show that care must be taken in using the configuration interaction model because of the significant intensity loss for all four anthracenophanes. For [2.2](9,10)AA this loss represents 65% of the intensity of two isolated (9,10)DMA molecules. Similar losses are also observed for the [2.*n*]-(9,10)anthracenophanes (III.G.3.), a result which reinforces the evidence from Figures 12 and 13. Clearly, these intensity losses provide a cautionary signal for contemplated theoretical approaches of these systems.

The very marked differences between the two sets of spectra in Figures 12 and 13 recall the spectra of the naphthalenophanes (III.D., Figures 10 and 11) and suggest a common interpretation, which probably involves the degree of overlap of the chromophores in the two types of cyclophanes. The *a*[2.2](1,4)AA and [2.2](1,4)(9,10)AA molecules each have a translation of one anthracene chromophore along the direction of the long molecular axis, compared with the other two anthracenophanes. An important effect of this translation is a reduction of the Coulombic repulsion term which raises the energies of the charge-transfer states. The intensities of the charge-transfer transitions will also be reduced, because these depend on the degree of overlap between donor and acceptor orbitals.

Considering the dimer states arising from the ^1L_a states of the two chromophores in the symmetrical overlapped sandwich conformation, we expect allowed transitions to $^1B_{2u}^+$ and $^1B_{2u}^-$ states (see II.E.). If the intensities of the localized and charge resonance transitions are comparable and the coefficients a and b are also comparable, there will be a cancellation of the two component intensities in the intensity of the $^1B_{2u}^-$ dimer state. In this situation only the $^1B_{2u}^+$ state will be observed. An analogous argument can be used for the two $^1B_{3u}$ states arising from the single molecule ^1B_b state. This interpretation can then account for the presence of only one band in the dimer spectra instead of two formally allowed bands from each of the two single-molecule bands.

For the dimer states of the two partially overlapped anthracenophanes it is reasonable that the intensities of the two localized (excitation resonance) transitions are larger than the intensities of the two charge resonance transitions, so that the moments no longer cancel and two bands are observed in each case.

There is some support for this qualitative interpretation of the data. For [2.2](9,10)AA Morita et al.[93] calculated that the $^1B_{2u}^+$ and $^1B_{2u}^-$ states should lie at 25 250 and 28 060 cm^{-1}, respectively, with calculated oscillator strengths of 0.19 and 0.008, respectively. For [2.2](1,4)(9,10)AA the corresponding values are 21 850 cm^{-1} (0.059) and 26 920 cm^{-1} (0.16), while for *a*[2.2]-(1,4)AA the values are 23 300 cm^{-1} (0.064) and 29 623 cm^{-1} (0.135). The situation is less clear for the states derived from ^1B_b as Morita et al.[93] invoked higher charge-transfer states to interpret some of the absorption bands.

Unfortunately the fluorescence polarization ratios measured by Morita et al.[93] do not provide unequivocal arguments to support definitive assignments. Measurements of linear polarization in single crystals are required to settle the assignments, and it should be possible to incorporate [2.2](1,4)(9,10)AA in single crystals of the photoisomer of 1,3-bis(9-anthryl)propane, which has an ideal crystal structure[94] to distinguish between short and long molecular axis polarizations for these molecules.

So far the question of conformational isomerism has not been raised because the room temperature solution spectra do not provide information about this aspect. However, a detailed study of the spectroscopy of [2.2](9,10)AA (see below) reveals the presence of two conformers, with quite different spectral and photochemical properties. The absorption spectrum of [2.2](9,10)AA in Figure 12 is due to a mixture of both conformers and it is not clear whether the solutions of the other anthracenophanes contain both conformers, or if not, which conformer is present. The theoretical calculations of Morita et al.[93] are based on overlapped conformations which are, most certainly, not the most stable conformation in each case.

3. [2.n](9,10)Anthracenophanes

Another set of anthracenophanes has been studied. These are the compounds [2.*n*](9,10)anthracenophane ([2.*n*](9,10)AA; n = 3–5),[95,96] which provide an array of conformational geometries particularly useful for the study of the photochemical behavior of the anthracene sandwich dimer as well as its spectroscopy. For the present case we concentrate on the latter aspects.

The solution absorption spectra of [2.*n*](9,10)AA (n = 2–5) are shown in Figure 14 along with their integrated oscillator strengths. We see that for all four compounds there is a marked loss of absorption intensity compared with that of the parent chromophore (9,10)DMA. This loss is greatest for n = 2 and least for n = 5. This observation reinforces the conclusion reached from a similar consideration of the spectra of the [2.2] anthracenophanes. The greater the overlap of the two chromophores in the sandwich conformation, the lower the integrated absorption intensity.

A comparison between the spectra of the four [2.*n*](9,10)AA anthracenophanes provides new insight into an analysis of the hypothetical sandwich dimer absorption spectrum. For n = 3–5 the bridge lengths are unequal so the short axes of each chromophore (neglecting the real departures from planarity which are present in these molecules) are not parallel. Concentrating on the four states derived from the lowest energy state of anthracene (^1L_a) we note that these are

$$^1B_{3g}^{\pm}: \qquad (a\Omega_+^1 \pm b\Pi_+^1)/\sqrt{(a^2+b^2)}$$

$$^1B_{2u}^{\pm}: \qquad (c\Omega_-^1 \pm d\Pi_-^1)/\sqrt{(c^2+d^2)}$$

If we denote the localized transition moment of each chromophore by $\mathbf{M}_\omega$ and the charge transfer moment by $\mathbf{M}_\pi$ and take θ as one half of the angle between the

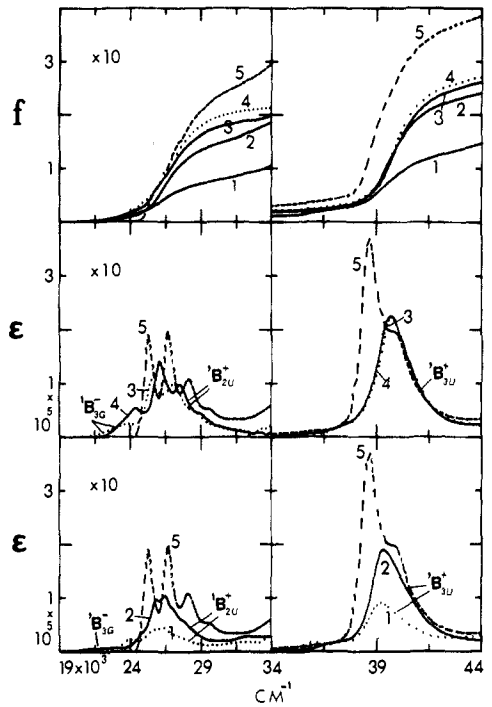

Figure 14. Bottom panels: Room-temperature solution molar absorption spectra (methyl cyclohexane) of [2.2](9,10)AA (1), [2.3](9,10)AA (2) and (9,10)DMA (5; 2 × ε). Middle panels: Room-temperature solution molar absorption spectra (methylcyclohexane) of [2.4](9,10)AA (3), [2.5](9,10)AA (4), and (9,10)-DMA (5; 2 × ε). Top panels: Corresponding oscillator strengths (f).

two short chromophore axes, then the intensities of the transitions to the two lowest energy states are

$^1A_g \rightarrow {}^1B_{3g}^-$:

$$4[[a^2M_\omega^2 + b^2M_\pi^2 - 2abM_\omega M_\pi] \sin^2\theta]/(a^2 + b^2)$$

$^1A_g \rightarrow {}^1B_{2u}^-$:

$$4[[c^2M_\omega^2 + d^2M_\pi^2 - 2cdM_\omega M_\pi] \cos^2\theta]/(c^2 + d^2)$$

The g and u subscripts have been retained to show the relationship to the sandwich dimer case. As $n \rightarrow 2$, $\theta \rightarrow 0$ and the absorption intensity to $^1B_{3g}^-$ goes to zero. However, the intensity of the transition to $^1B_{2u}^-$ only goes to zero if $\mathbf{M}_\omega = \mathbf{M}_\pi$ and $c = d$. We therefore expect to see two absorption bands which are much weaker than the main band ($^1A_g \rightarrow {}^1B_{2u}^+$), at lower energies than it, whose intensities drop from $n = 5$ to $n = 3$, and only one band for $n = 2$. Furthermore, the polarization of these two bands should be orthogonal, the higher energy band has its transition moment parallel to the mean short chromophore axis while the lower energy band has its moment normal to the mean chromophore plane.

These expectations are borne out by experiment. First we examine the polarized single-crystal absorption spectrum of [2.4](9,10)AA which is shown in Figure 15 in the upper panel along with a projection of the molecule onto the crystal face.[97] The extinction directions are parallel and perpendicular to E and we see that these directions distinguish between the long molecular axis (projects very strongly $\perp E$) and the other two anthracenophane axes (which both project strongly $\|E$). The lower panel in Figure 15 shows the polarized absorption spectrum of a single crystal of the photoisomer of [2.4](9,10)AA containing a small amount of [2.4]-(9,10)AA. In this lattice the polarization direction X detects the long molecular transition moment while the Y direction detects the other two molecular axis transition moments.

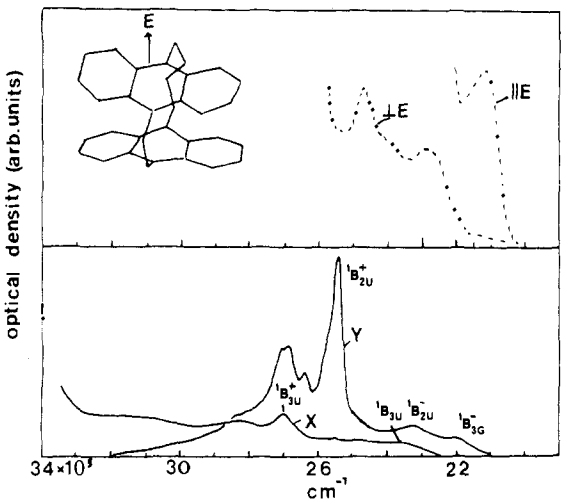

Figure 15. Absorption spectrum of [2.4](9,10)AA at 10 K (top panel) in its single crystal with the projection of the molecule shown in the inset. The 10 K absorption spectrum of [2.4](9,10)AA in its photoisomer as a host crystal is shown in the lower panel. The X spectrum is polarized parallel to the long axis of the molecule while the Y spectrum is polarized parallel to the short molecular axis.

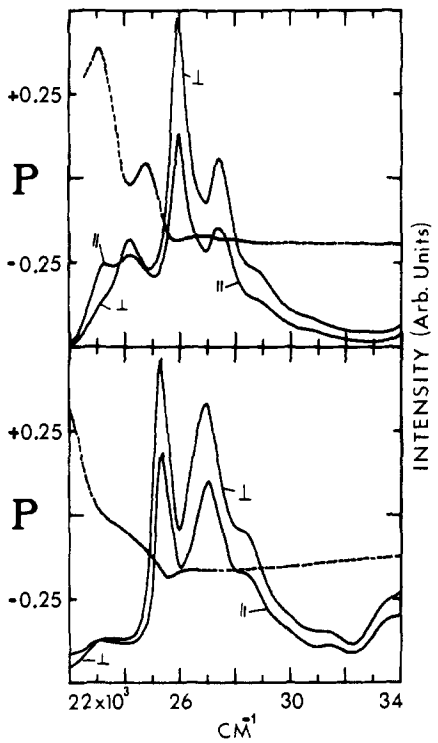

Figure 16. Lower panel: Polarized corrected fluorescence excitation spectra of [2.4](9,10)AA in methylcyclohexane–isopentane (1:3) at 100 K, 90° configuration, parallel (‖) and perpendicular (⊥) to the exciting radiation. The polarization ratio (P) is shown by the broken curve. Upper panel: Same for [2.5](9,10)AA.

We see from the upper panel of Figure 15 that the lowest energy absorption band in pure [2.4](9,10)AA has E polarization so the transition moment direction lies either along the short chromophore axis or the middle axis (normal to the mean chromophore plane). The

next higher energy region has mixed polarization in the pure crystal. There is a weak $\perp E$ absorption and a much stronger $\parallel E$ absorption. The mixed polarization of this region is shown more clearly in the lower panel of Figure 15.

In order to resolve the polarization direction of the major component of the second absorption band of [2.4](9,10)AA we take advantage of the fluorescence properties of this material by measuring the polarization ratio of the fluorescence in a rigid glass.[97] The polarized excitation spectra and the polarization ratio are shown in Figure 16, and we see that the second absorption band ($\sim$23 000 cm^{-1}) has a strong perpendicular component and thus has its transition moment in an orthogonal direction to that of lowest energy absorption band. Although the crystal and rigid glass polarization data cannot determine the actual polarization directions in the chromophore, they do support the theoretical expectation of orthogonal polarizations for the two bands.

The assignments are further supported from the fluorescence polarization ratios obtained from [2.5]-(9,10)AA in a rigid glass also shown in Figure 16. For this molecule the angle θ is larger and the intensities of both bands are larger than for the spectrum of [2.4](9,10)AA, as expected. The orthogonal polarization of the two lowest energy bands is more apparent for this compound.

The absorption spectra of [2.n](9,10)AA support the theoretical expectations for the sandwich dimer in the observation of three of the possible four states arising from the ^1L_a single molecule state. The fourth state, $^1B_{3g}^+$ should lie above $^1B_{2u}^+$, but as it will be overlapped by the much more intense absorption to this latter state, it cannot be detected.

The single-crystal polarized absorption spectra shown in Figure 15 also provide information about the states derived from the single molecule ^1L_b state which cannot be obtained from measurements in solution or rigid glasses.

There are four dimer states arising from this molecular state

$$^1B_{2g}^{\pm}: \qquad (a\Omega_+^2 \pm b\Pi_+^2)/\sqrt{(a^2+b^2)}$$

$$^1B_{3u}^{\pm}: \qquad (c\Omega_-^2 \pm d\Omega_-^2)/\sqrt{(c^2+d^2)}$$

For the [2.n](9,10)AA absorption spectra the absorption intensities to the two g states will be zero because the long chromophore axes are effectively parallel in each case. This leaves the two u states which are seen in the X polarization of the lower panel of Figure 15 for [2.4](9,10)AA. The more intense band system has its origin at 27 000 cm^{-1} while the lower state occurs as the broad band at 23 500 cm^{-1} in the same polarization. Both bands are observed for all four compounds although the lower energy band is very weak for [2.2]-(9,10)AA indicating, as for the analogous $^1B_{2u}^-$ band, that localized and charge transfer intensities are not quite equal.

Examination of the principal features of the absorption spectra of the [2.n](9,10)anthracenophanes in the visible and near ultraviolet have provided assignments which are in very good qualitative agreement with the predictions of theory. Five of a possible eight states arising from ^1L_a and ^1L_b have been identified and assigned. The quantitative agreement between theory and experiment is not good, but, given the nature of the approximations used, the discrepancies are easily understood. The analysis has also shown that the localized and charge-resonance transition moments are of comparable magnitude for [2.2](9,10)AA, which supports the analysis of the absorption spectra of the various [2.2]anthracenophanes given above.

It has been assumed in the above analysis that the X polarized absorption in Figure 15 belongs to transitions to states derived from the ^1L_b state of anthracene. We note that the origin band of the transition $^1A_g \rightarrow {}^1B_{3u}^+$ lies about 1500 cm^{-1} to higher energy than the origin band of the transition $^1A_1 \rightarrow {}^1B_{2u}^+$, which raises the possibility of a vibronic assignment (intensity stealing from the higher energy ^1B_b state), considered in some detail by Michl et al.[54] Also, the origin of the transition $^1A_g \rightarrow {}^1B_{3u}^-$ lies about 1500 cm^{-1} to higher energy of the $^1A_1 \rightarrow {}^1B_{3g}^-$ transition. The polarizations require a b_{1g} vibration in the first case and an a_u vibration in the second case, for the dimer. Both of these vibrations would then be derived from the b_{1g} vibration of the anthracene chromophore proposed by Michl et al.,[54] and the assignment is therefore feasible on polarization grounds. Its main difficulty comes from the relatively large intensity of the lower energy ($^1B_{3u}^-$) band in comparison with the higher energy band ($^1B_{3u}^+$), suggesting a more effective vibronic mixing induced by the a_u dimer vibration than is the case for the b_{1g} vibration. It must still, however, be considered a serious alternative assignment, especially as it removes some of the difficulties in understanding the long-axis polarized absorption in the anthracenophane absorption spectra.

4. Conformational Aspects

Whereas paracyclophane appears to have only one stable conformation, [2.2](9,10)AA occurs with two distinct conformations. The α crystal form has the rotated conformation in a disordered crystal structure[95] while the β crystal has the translated conformation.[98] Molecular mechanics calculations indicate that the rotated conformer is the more stable.[95]

[2.2](9,10)AA present as a guest in crystals of its own photoisomer shows a temperature dependence of its absorption spectrum which suggested a temperature-dependent equilibrium between the two conformations in the crystal site.[97] Similarly, the absorption spectrum in solution[93] shows pronounced intensity changes on cooling which are again suggestive of a conformational equilibrium.

A detailed study of the spectroscopy and photochemistry of [2.2](9,10)AA in crystals has been made which used a method of selective photochemistry to isolate each conformer at liquid helium temperatures.[95] This involved the incorporation of the photoisomer as a guest in single crystals of the photoisomer of 1,3-bis(9-anthryl)propane, followed by a few minutes of heating to about 50 °C to decompose some of the [2.2](9,10)AA photoisomer to form both open conformers. It was found that at liquid helium temperatures each conformer is trapped in the crystal, and irradiation with monochromatic light at 417 nm or 399 nm leads to the selective photoisomerization of the translated or rotated conformer, respectively. The photoselection is

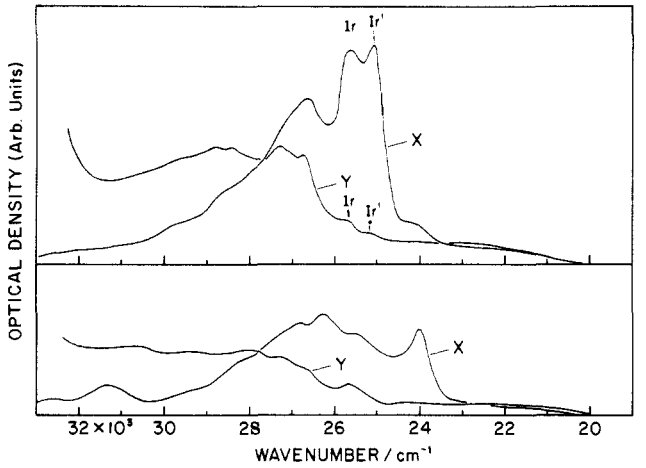

Figure 17. Absorption spectra at 8 K of the rotated (top) and translated (bottom) conformers of [2.2](9,10)AA in a single crystal of 1,3-bis(9-anthryl)propane photoisomer for light incident on the (010) crystal face.[95] *r* and *r'* correspond to two orientations of the molecule in the site.[120] The short and long molecular axes project onto the *X* and *Y* polarization directions, respectively.

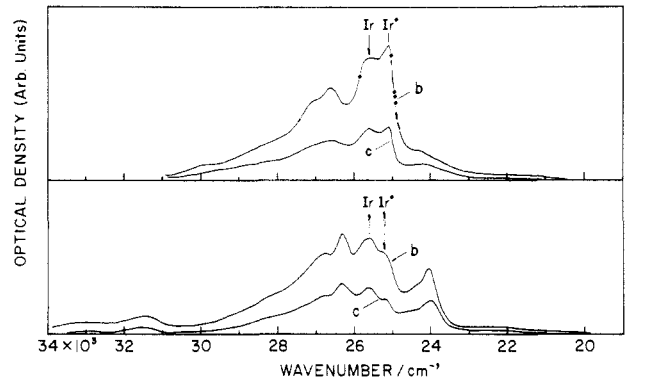

Figure 18. Same as for Figure 17 but for light incident normal to the (100) crystal face. b and c are for light polarized parallel to the crystal *b* and *c* axes, respectively, and they both contain projections of the short molecular axis.

not perfect because of some spectral overlap, but it is very good. In order to establish the identity of the conformers, the relative rates of photoisomerization were determined under identical conditions. It was found that one species photoreacted 4 to 5 times faster than the other so it was assigned to the rotated conformer because it is related topochemically to the photoisomer through their similar bridging methylene conformations.

Although the photoselection allows the preparation of either conformer the resulting individual spectra appear to represent the absorption by two slightly different orientations of each conformer in the sites. The relevant spectra are given in Figures 17 and 18.

We see that the absorption spectra of the two conformations are quite different. The spectrum of the translated conformer suggests that the intensities of the localized and charge resonance transitions are no longer comparable and the band at 24 000 cm^{-1} would then represent the $^1B_{2u}^-$ state, which is also displaced to higher energy because the energy of the charge resonance has also been moved upwards in energy because of the translation of one chromophore over the other. These marked differences between the absorption spectra of the two conformers represent a challenge for theory.

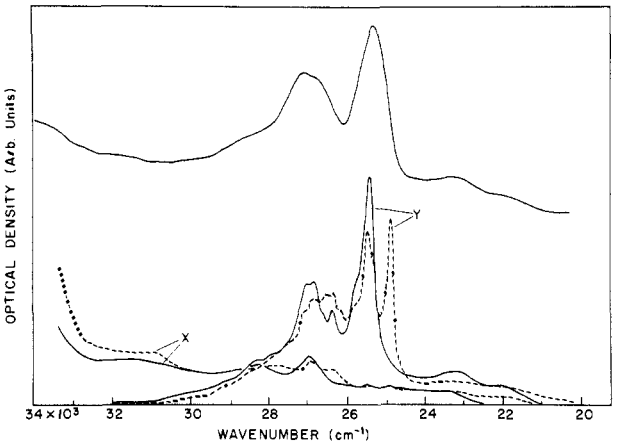

Figure 19. Bottom curves (*X* and *Y*) show the 8 K polarized absorption spectra of [2.4](9,10)AA in its photoisomer crystal, obtained after 8 K photocleavage of the photoisomer (broken curves) and after heating the crystal to about 100 K for a few seconds and cooling to 8 K (full curves). The long and short molecular axes project onto the *X* and *Y* crystal polarizations, respectively. The top curve shows the room-temperature solution (methylcyclohexane) absorption spectrum.

[2.3](9,10)AA has two calculated conformers,[95] one rotated and the other translated, with respect to the symmetrical overlapped conformation. Comparison of solution and crystal spectra show that both conformers are present, to varying extents in each case, but attempts at selective photochemistry failed.

[2.4](9,10)AA has four calculated conformers.[96] Compared with an hypothetical eclipsed conformation, one conformation displays a small relative rotation of one anthracene chromophore about the interchromophore axis (*r*) while the other shows a small relative translation parallel to the long molecular axis (*t*). The number of these pairs (a and b) is determined by the number of possible conformations of the four carbon atom bridge (as constrained by the 1,2-bis(9-anthryl)-ethane framework). X-ray structure determination shows that the a*r* and a*t* conformations occur in the crystal,[96] consistent with their greater calculated stability. However, the absorption spectroscopy measurements either in solution (Figure 14), rigid glass (Figure 16), or single crystals (Figure 15) do not indicate more than one conformer and all spectra suggest that this is the a*r* conformation.

[2.4](9,10)AA shows fluorescence, and the temperature dependence of the emission suggests that the initial conformer (a*r*), reached by absorption of light, relaxes to a*t*, which has a shorter contact distance between opposite C(10)···C(10') atoms on each chromophore. The excimer emission profile shifts to lower energy as result of the relaxation, which occurs on softening at rigid glass. Above about 200 K there is a drop in the fluorescence yield and a shift of the excimer maximum by about 3000 cm^{-1} to lower energy, and photoisomerization takes place. These changes are consistent with a further relaxation to b*t* (fluorescent) and b*r* (nonfluorescent and photoreactive).

Photodissociation of single crystals of the photoisomer of [2.4](9,10)AA produces [2.4](9,10)AA, and if this is carried out at about 10 K, a mixture of a*r* and b*r* conformations is obtained, the relative amounts being sample dependent because of differences in internal inhomogeneity. The b*r* conformer is nonfluorescent, and it is photochemically and thermally labile.

At 10 K the br conformation can be photoisomerized while heating the sample to about 100 K for a few seconds transforms it to the ar conformation (see Figure 19).

Theoretical calculations for [2.5](9,10)AA show a set of six conformations and the crystal structure is consistent with the presence of the two with the largest C(10)···C(10′) contact distance (about 4.5 Å). The two conformations with the highest energy have C(10)···C-(10′) contact distances of about 3.9 Å. The lack of photoisomerization is probably linked to the inability of the excited complex to reach one or both of these conformations because of the high barriers to internal rotations of the pentane bridge.

F. Pyrenophanes

As pyrene provided the original aromatic excimer there has been interest in the synthesis of pyrenophanes. In spite of the difficult chemistry a surprising number of different molecules have been made but, as yet, spectroscopic data and analysis are meager.

The most symmetrical compound [2.2](2,7)pyrenophane was reported first by Umemoto et al.[99] and subsequently by others.[100,101] Its molecular structure has been determined[102] by X-ray methods as has the structure of a 1,1′-diene derivative.[103]

[3.3]- and [4.4](2,7)pyrenophanes have been prepared by Staab et al.[104] and their molecular structures determined by X-ray methods. The reports of their electronic spectroscopy are limited to the wavelengths of maximum absorption in the solution absorption spectra, a spectral profile of the fluorescence of [4.4](2,7)pyrenophane in 2-methyltetrahydrofuran at 1.3 K, and the fluorescence maxima and emission half widths in crystals and MTHF at 1.3 K.

Kawashima et al.[105] have reported the synthesis and spectroscopic properties of three other [2.2]pyrenophanes: [2.2](1,6)PP, [2.2](1,6)(2,7)PP, and [2.2]-(1,8)PP. Umemoto et al.[106] have given the synthesis and absorption spectrum of [2.2](1,3)pyrenophane.

[2.2](1,8)PP can exist in syn and anti isomeric forms but the NMR data indicated the presence of only the anti isomer. In contrast to the symmetrical overlapped conformation of [2.2](2,7)PP, both [2.2](1,6)PP and [2.2](1,6)(2,7)PP have smaller overlaps, particularly the former. In view of the observations made for the naphthalenophanes and anthracenophanes it is not surprising that there are substantial differences between the spectra of [2.2](2,7)PP and those of [2.2](1,6)PP and [2.2](1,6)(2,7)PP. The absorption spectra of all four compounds are shown in Figure 20 for the near ultraviolet and visible regions together with the spectrum of pyrene.

The integrated absorption intensities are also given in Figure 20, and it can be seen that, as for the anthracenophanes, there is a decrease of absorption intensity compared with that of pyrene. However, the most interesting aspect of the spectra is the apparent redistribution of absorption intensity, which provides the lower energy region with enhanced intensity at the expense of the higher energy band. This behavior is very similar to that observed for the anthracenophanes and the naphthalenophanes discussed in III.D.,E. It suggests that for the symmetrical [2.2](2,7)PP the localized and charge resonance transition moments have

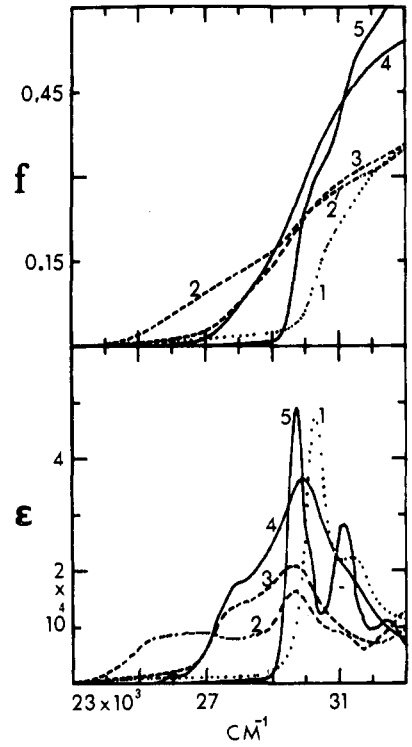

Figure 20. Lower panel: Room-temperature solution molar absorption spectra[105] of [2.2](2,7)PP (1), [2.2](1,6)PP (2), [2.2](1,6)(2,7)PP (3), [2.2](1,6)(2,7)PP (4), and pyrene (5; 2 × ε). Upper panel: Corresponding oscillator strengths (f).

similar intensities, but if the degree of overlap is reduced, the charge resonance transition moment is smaller and the absorption intensity becomes more evenly distributed between the two allowed transitions. Clearly, more detailed spectroscopic data are required for these very interesting compounds.

G. Heterophanes and Mixed Cyclophanes

1. Introduction

A number of remarkedly interesting heterophanes and mixed cyclophanes have been prepared by Misumi and co-workers. The first two of these to be described were the *syn*- and *anti*-[2.2](1,4)naphthaleno(1,4)-anthracenophanes (*s*[2.2](1,4)NA and *a*[2.2](1,4)NA).[87] They reported their room-temperature absorption spectra, but they found these spectra too difficult to interpret.

A very important paper[107] describing the preparation and spectral properties of [2.2]naphthaleno- and [2.2]anthracenoheterophanes was preceded by another dealing with layered paracycloheterophanes.[108] In each case the hetero compound included either furan or thiophene. In both cases Otsubo et al.[107,108] noted that the thiophene ring interacts more strongly with the condensed aromatic ring than the furan ring. The spectra of the heterophanes were also compared with the spectra of the corresponding mixed paracyclophanes prepared earlier.[109]

A later paper[88] reported a comparison of the properties of all possible mixed cyclophanes containing anthracene with naphthalene and benzene, bridged at either the (1,4) or (9,10) positions of the anthracene molecule.

It is not relevant to review the properties of the heterophanes and mixed cyclophanes which have multi

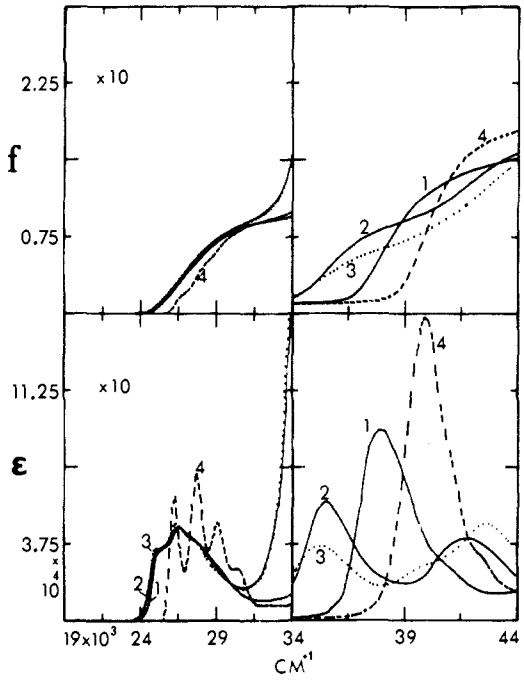

Figure 21. Lower panels: Room-temperature solution molar absorption spectra[107] of [2.2](1,4)AF (1), [2.2](1,4)ATh (2), [2.2](1,4)APC (3), and (1,4)DMA (4). Upper panels: Corresponding oscillator strengths (f).

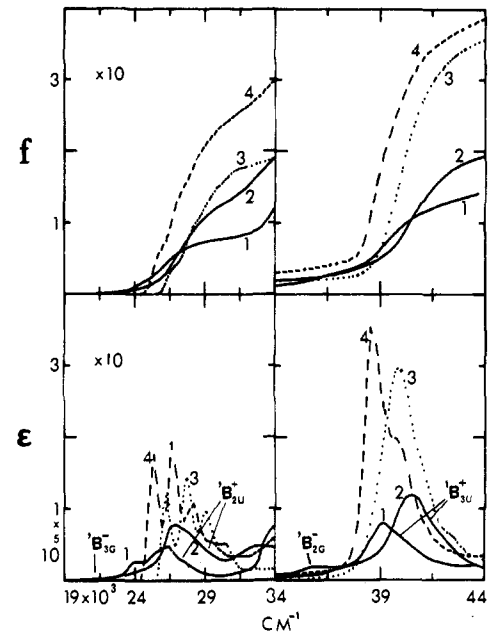

Figure 22. Lower panels: Room-temperature solution molar absorption spectra[107] of [2.2](9,10)AF (1), [2.2]((,10)ATh (2), [2.2]((9,10)APC (3), and (9,10)DMA (4). Upper panels: Corresponding oscillator strengths (f).

layers so the present discussion is limited to the two-layer systems.

2. Heteroanthracenophanes

The absorption spectra of the four heteroanthracenophanes [2.2](1,4)anthraceno(2,5)furanophane ([2.2](1,4)AF), [2.2](9,10)anthraceno(2,5)furanophane ([2.2](9,10)AF), [2.2](1,4)anthraceno(2,5)thiophenophane ([2.2](1,4)ATh), [2.2](9,10)anthraceno(2,5)thiophenophane ([2.2](9,10)ATh), the two related anthracenoparacyclophanes, and the two anthracene chromophores and their integrated absorption intensities are shown in Figures 21 and 22.

The striking feature of the spectra in Figures 21 and 22 is the pronounced difference between the thiophenophane and furanophane spectra in the region above about 32 000 cm^{-1}. The spectrum of each of the furanophanes is obviously very closely related to the spectrum of the respective anthracene chromophore, so far as band shape is concerned.

The absorption spectrum of furan has a band with maximum at 46 410 cm^{-1} (ϵ = 5010) while for thiophene the corresponding value is 43 290 cm^{-1} (ϵ = 5890).[110] The bands lie above the position of the intense ^1B_b band of the anthracene chromophore (38 680 cm^{-1}), but the interaction between the two chromophores can be considerable even though they are not identical (case 3 in II.A.). A nonzero value for the excitation exchange integral is required and this means that the two transition moments must be parallel for the dipole–dipole term to be nonzero.

There has been a substantial amount of theoretical work related to the electronic structures of furan and thiophene.[111,112] In each case the lowest energy $\pi-\pi^*$ transitions are to $^1A_1$ and $^1B_1$ states, but the relative order is open to question. It appears likely that the transition intensity to $^1B_1$ is considerably larger and the position of the $^1A_1$ state is therefore not certain in each spectrum. As the transition moment of the transition to $^1A_1$ lies parallel to the long axis of the anthracene chromophore in the heterocyclophane, it will be this state which interacts with the ^1B_b state of the anthracene chromophore. It has to be assumed that for furan the $^1A_1$ state lies above the $^1B_1$ state, while for thiophene the reverse is true.

We note from Figures 21 and 22 that, even neglecting the intensity of the thiophene chromophore, the integrated intensities of the heterophanes are less than that of the isolated anthracene chromophores, but the difference is smaller for the (1,4) bridged compound as might be expected. We note also the similarity between the spectra of the anthracenoparacyclophanes and the anthracenothiophenophanes, indicating a similarity between the energy levels of thiophene and benzene.

Otsubo et al.[107] observed fluorescence from all compounds but gave no details other than the positions of the fluorescence maxima at room temperature in solution.

3. Benzene–Anthracene Cyclophanes

The absorption spectra of [2.2](1,4)anthracenoparacyclophane ([2.2](1,4)APC) and [2.2](9,10)anthracenoparacyclophane have been reported by Otsubo et al.[107] and Iwama et al.[88] while the absorption and fluorescence spectra of [2.2](9,10)anthracenometacyclophane ([2.2](9,10)AMC) and [2.2](9,10)APC have been studied by Ferguson et al.[113]

The spectra of [2.2](9,10)APC, [2.2](9,10)AMC, and (9,10)DMA are shown in Figures 23 with their integrated absorption intensities. We note the striking difference between the spectra of the two cyclophanes. The spectrum of [2.2](9,10)AMC is similar to that of [2.2](9,10)AF (Figure 22) while that of [2.2](9,10)APC is similar to that of [2.2](9,10)ATh.

The calculated molecular structures of the most stable (and probably the only) conformer of each molecule are shown in Figure 24. We see that for [2.2](9,10)-

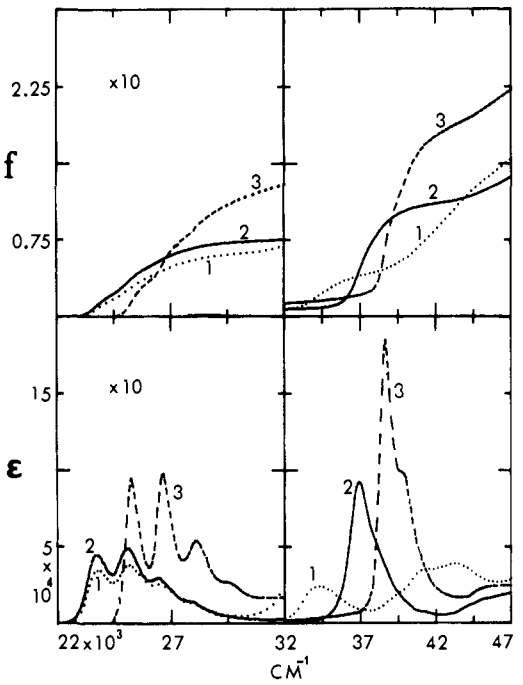

Figure 23. Lower panels: Room-temperature solution molar absorption spectra[113] of [2.2](9,10)APC (1), [2.2](9,10)MPC (2), and (9,10)DMA (3). Upper panels: Corresponding oscillator strengths (f).

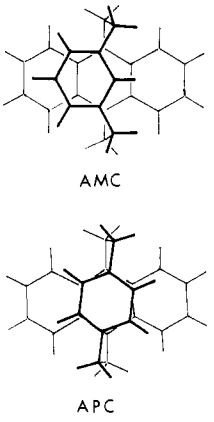

Figure 24. Calculated molecular structures of the stable conformations of [2.2](9,10)APC and [2.2](9,10)MPC.[113]

AMC the transition moment for the ^1B_b state of the anthracene chromophore is exactly orthogonal to the transition moment of the ^1L_b state of the *m*-xylene chromophore. Therefore the dipole–dipole contribution to V (case 3 in II.A.) is zero, so even though there is near degeneracy of these two states, tan $\gamma \approx 0$ and the eigenfunctions of the dimer are essentially pure individual chromophore functions. On the other hand for [2.2](9,10)APC the dipole–dipole contribution to V is nonzero because the respective moments are parallel. Tan $\gamma \gg 1$ and both dimer functions have significant amounts of ^1B_b so the absorption intensities to the two (split) states are comparable (see Figure 1). The polarization of each of the transitions to these states will be parallel to the long chromophore axis, and this polarization for the lower energy band has been confirmed by polarized single-crystal spectroscopy as well as from measurements of the fluorescence polarization ratio in a rigid glass.

As might be expected from the absorption spectra the fluorescence spectra of both [2.2](9,10)APC and

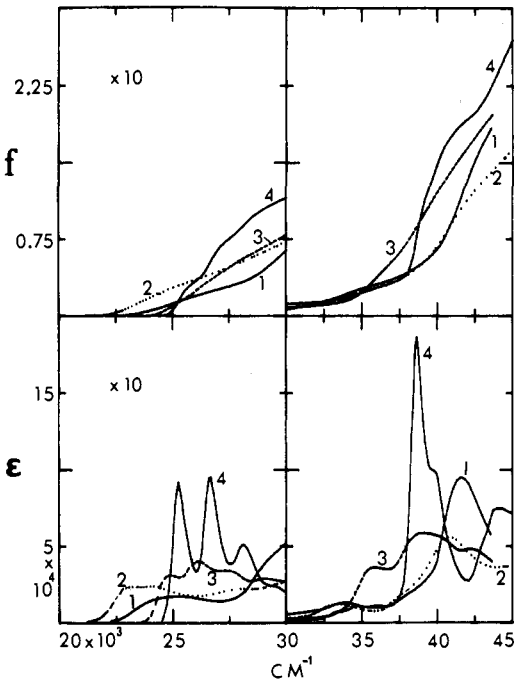

Figure 25. Lower panels: Room-temperature solution molar absorption spectra[88] of *s*[2.2](1,4)NA (1), [2.2](1,4)N(9,10)A (2), *a*[2.2](1,4)NA (3), and (1,4)DMN + (9,10)DMA. Top panels: Corresponding oscillator strengths (f).

[2.2](9,10)AMC show good overlap and have vibrational structure even at room temperature.

The absorption spectrum of [2.2](1,4)APC is similar to that of [2.2](1,4)ATh as expected.

4. Heteronaphthalenophanes

The absorption spectra of [2.2](1,4)naphthaleno(2,5)furanophane ([2.2](1,4)NF) and the syn and anti isomers of [2.2](1,4)naphthaleno(2,5)thiophenophane ([2.2](1,4)NTh) have been reported by Otsubo et al.[107]

As for the analogous anthracene compounds the absorption spectrum of [2.2](1,4)NF resembles that of 1,4-dimethylnaphthalene (DMN) except that the ^1B_b and ^1L_a bands are shifted to lower energy and there is an overall loss of intensity. Similarly the two thiophene compounds show two bands instead of the ^1B_b band, and the same is true for the absorption spectrum of [2.2](1,4)naphthalenoparacyclophane. Room-temperature fluorescence maxima were also reported.

The interpretation of the spectra of these compounds follows in analogous fashion to those of the corresponding anthracene compounds. The lowest energy state of the naphthalene chromophore, ^1L_a, shifts to lower energy because of the proximity of the thiophene or furan chromophore. For the ^1B_b state, however, there is a strong interaction with a near degenerate state in thiophene which produces a splitting, and the absorption intensity associated with the ^1B_b band is shared between the two bands of the dimer. For furan this near degeneracy is absent, and the absorption spectrum resembles that of the naphthalene chromophore.

5. Naphthalene–Anthracene Cyclophanes

The absorption spectra of [2.2](1,4)naphthaleno(9,10)anthracenophane ([2.2](1,4)N(9,10)A), *s*[2.2](1,4)NA, and *a*[2.2](1,4)NA, reported by Iwama et al.[88] are shown in Figure 25. As for the other cyclophanes there is an overall loss of intensity over the whole

spectral region, compared with the intensities of the individual chromophore spectra. We might expect that the spectra of [2.2](1,4)N(9,10)A and *s*[2.2](1,4)NA would be similar because the overlaps of the two chromophores are similar, neglecting possible differences in conformations. The room-temperature spectra do not allow a full assessment of the spectral comparisons in the region related to the ^1L_a states, but it does appear from the region of 30 000–45 000 cm^{-1} that this expectation is borne out for the ^1B_b states.

An analysis can be made by using case 3 of the simple model (Figure 1). For *s*[2.2](1,4)NA E_1^2 = 41 600 cm^{-1} and E_2^2 = 33 700 cm^{-1} while for [2.2](1,4)N(9,10)A E_1^2 = 40 600 cm^{-1} and E_2^2 = 33 200 cm^{-1}. Assuming that $\Delta D^2 \ll \Delta E^2$, we have ΔE^2 = 5300 cm^{-1} for the individual monomers (DMN and (9,10)DMA). The E_1^2–E_2^2 separation in the two cyclophanes is about 7700 cm^{-1}, and the ratio of this value to ΔE^2 provides us with $\Delta E^2 = 2V$ (see Figure 1), so that V = 2650 cm^{-1}. The theoretical intensity ratio for the two bands in the cyclophane (assuming equal monomer intensities) is 5.7 (see Figure 1) which agrees well with experiment. We note in passing that the cyclophane bands are shifted to lower energy from their calculated positions (E_1^2 lies lower than the ^1B_b state of DMN, Figure 25). This is because the repulsion energies inherent in the strained molecule raise the ground-state energies of the two chromophores.

If the simple model is to be useful, then it must be able to account for the different spectrum observed for *a*[2.2](1,4)NA. Calculations of V are required for the different geometries, but there is no doubt that V will be less for *a*[2.2](1,4)NA than for *s*[2.2](1,4)NA. The two states E_1^2 and E_2^2 will lie closer in energy and, importantly, the intensity of the lower energy band will grow at the expense of the higher energy band. The observed spectrum (Figure 25) shows qualitative agreement with these expectations (a value of $\Delta E^2 \approx 4V$ in Figure 1 would match the observed intensities reasonably well), but the data are really insufficient to allow a definitive assignment. Clearly more spectroscopic work needs to be carried out with these compounds.

So far there appears to be no need to consider charge-transfer bands for an analysis of the spectra of the mixed and heterocyclophanes. The spectral changes seem to be adequately handled by the coupled chromophore model of case 3, but this simple approach ignores the definite overall loss of intensity, compared with the sum of the individual chromophore intensities, characteristic of the spectra of all the cyclophanes. As a sharper focus is obtained through the availability of low-temperature data, especially from crystalline media with polarized light, the deficiencies of the simple model will become apparent.

A start has been made in this direction through spectroscopic studies of [2.2](1,4)N(9,10)A[113] and 1,2,3,4-tetrahydro[2.3](9,10)anthracenophane[114] ([2.3]-AAH_4), which is a mixed cyclophane of naphthalene and anthracene chromophores. The room-temperature solution absorption spectra of both compounds as well as the sum of (1,4)DMN and (9,10)DMA spectra together with their integrated absorption intensities are given in Figure 26. The positions of the two sets of bands associated with the ^1L_a states of the two chromophores

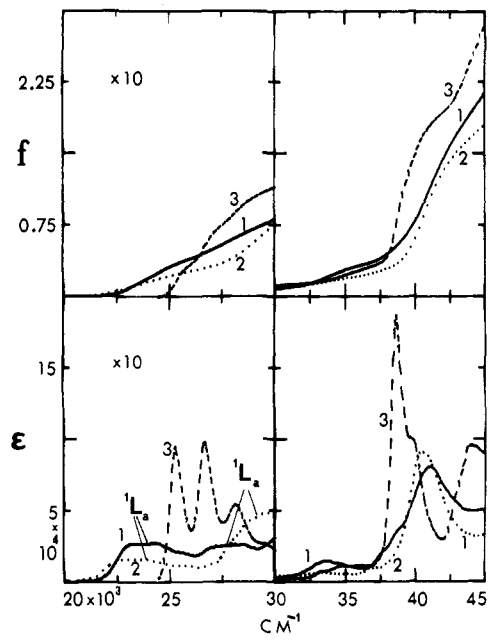

Figure 26. Lower panels: Room-temperature solution molar absorption spectra[113,114] of [2.2](1,4)N(9,10)A (1), [2.3]AAH_4 (2), and (1,4)DMN + (9,10)DMA. Top panels: Corresponding oscillator strengths (f).

are indicated in Figure 26 and these assignments have been confirmed by polarized single-crystal measurements. Both of these states undergo a red shift, compared with their positions in the spectra of the monomers, with that for the naphthalene chromophore being the larger. Whereas these two states are separated by about 8000 cm^{-1} in DMN and (9,10)DMA, the separation is about 4000 cm^{-1} for [2.2](1,4)N(9,10)A and about 6000 cm^{-1} for [2.3]AAH_4. This behavior is incompatible with case 3 of the simple model. Another disturbing feature of the spectra is the intensities of these two bands in the cyclophane spectra. The transition to the ^1L_a state of the anthracene chromophore has oscillator strengths of 0.025 ([2.3]AAH_4) and 0.04 ([2.2](1,4)N-(9,10)A) compared with 0.12 for (9,10)DMA. The lengthening of the fluorescence decay time in [2.3]AAH_4 and the sandwich dimer of ANP is consistent with this reduction of absorption intensity of the ^1L_a band. The intensity of the ^1L_a band of the naphthalene chromophore in the spectrum of (1,4)N(9,10)A is somewhat less than for the ^1L_a band in the (1,4)DMN spectrum whereas it is considerably reduced for [2.3]AAH_4. All of these effects are difficult to reconcile with the apparent success of the simple model in interpreting the features of the states derived from the ^1B_b states of the two chromophores.

The absorption band at 33 000 cm^{-1} in the spectrum of [2.3]AAH_4 was assigned[114] to a charge transfer transition on the basis of its polarization in single crystal measurements. The analogue of this band in the spectrum of [2.2](1,4)N(9,10)A is more intense (Figure 26), and it has a predominant polarization parallel to the long axis of the chromophores, consistent with its assignment to the E_2^2 component of the two interacting ^1B_b states given above. It might be expected that the increase of one CH_2 group to one bridge in [2.3]AAH_4 would lower V slightly, thereby moving intensity out of the E_1^2 band into the E_2^2 band, but this is not observed. Obviously, more spectroscopic work needs to be carried out with these systems.

IV. Sandwich Dimers

A. Introduction

Initially,[1,2] sandwich dimers were produced by photocleavage of photodimers in a rigid glass matrix such as methylcyclohexane at 77 K. It was always clear that as a glassy matrix has an inhomogenious micro structure the relative arrangement of the two molecules is subject to considerable variation. For example, irradiation with 365-nm light after production of sandwich dimers of anthracene at 77 K leads to a rephotodimerization of only a few percent of the sandwich dimers in the glass. Only a small fraction of the pairs of molecules can return photochemically to the photodimer, and the majority of the sandwich dimers are far from the expected symmetrical sandwich dimer configuration. Furthermore, experiments indicated that for anthracene the sandwich dimer is unstable in the ground state, and the preferred arrangement is similar to that found in the unit cell of the crystal.

Morris[115] and Chandra and Sudhindra[116] made independent theoretical investigations of the structure of anthracene dimers. Chandra and Sudhindra[116] concluded that both anthracene and naphthalene should form weak, but stable, sandwich dimers, and they found further that the orientation, deduced from analysis of the stable dimer spectrum of anthracene,[3] is unstable. Morris[115] tackled the same problem and found that an atom–atom potentials method gave the sandwich dimer as the most stable arrangement for two anthracene molecules, in agreement with Chandra and Sudhindra.[116] As this result was contrary to experiment he examined another approach which involved the separate evaluation of the several terms which make up the intermolecular potential. He found that quadrupole–quadrupole interactions, previously neglected, are dominant and they provide a repulsive term for the sandwich dimer, but become attractive for rotations away from this configuration. There is additional support for the conclusion of Morris[115] from the work of Califano et al.[117] who included quadrupole–quadrupole interactions in the calculations of the lattice dynamics of naphthalene, obtaining for the first time the correct ordering of the highest A_g and B_g lattice modes.

Clearly, a more homogeneous environmental cage is required for the dissociated photodimer, and it is natural to consider the use of crystals, such as the parent photodimer, to replace the rigid glass. Additional constraints on the sandwich dimer are provided by chemical bridges using coupled chromophores which photoisomerize. Their photodissociation can then be carried out in a rigid glass or in a host crystal to provide sandwich dimers for spectroscopic study. The present section deals with these aspects.

B. Sandwich Dimers From Photodimers

The original reports of Chandross et al.[1-3,5] dealt with the sandwich dimer of anthracene as well as those of 9-methyl, 9-chloro-, and 9-bromoanthracene, considered as "symmetrical" dimers. Spectral analysis was made using the FG vibronic coupling model. The derived excitation exchange integrals for the ^1L_a state range from 250 to 400 cm^{-1} while those for the ^1B_b state vary from 1350 to 1700 cm^{-1}. These are lower but in overall reasonable agreement with the calculated values of 730 and 2600 cm^{-1} for ^1L_a and ^1B_b, respectively, for a symmetrical anthracene sandwich dimer separated by 3.5 Å based on the distributed transition dipole method and scaled to the experimental intensity.[25]

The same sandwich dimers were reexamined by Ferguson et al.,[118] and more attention was paid to the effects of controlled softening of the glass on the absorption and emission spectra. The observations suggest that the dimer dissociates by simply moving apart while undergoing a small rotation of one molecule relative to the other about the intermolecular axis. The effect of softening on the emission spectrum was also studied for the 9-chloroanthracene sandwich dimer. The initial, very broad, excimer emission with a decay time of 180 ns is replaced by a less red-shifted excimer with a decay time of about 100 ns. There is then a sudden change to a broad emission showing some vibrational structure and a short decay time of about 5 ns. Finally, the characteristic monomer emission appears with a decay time of 10 ns.

A feature of the absorption spectra of all of the sandwich dimers in the region of the lowest energy absorption band (derived from ^1L_a) is their intensity distribution. Unlike the monomer spectrum the Franck–Condon maximum lies in the second peak. Also, the maxima all lie to lower energy (by about 250 cm^{-1}) from the corresponding maxima of the monomer spectrum. The altered intensity distribution was interpreted by Chandross et al.[3] within the framework of the FG vibronic coupling model. However, Morris[25] used a weak coupling model to account for this feature. The red shift of the dimer band system comes from a change in the dispersion energy and static interaction energy between the two molecules when one is electronically excited. There must also be a contribution from a destabilization of the ground state by repulsion forces if the environmental cage maintains an interchromophore separation below the van der Waals distance. This total shift is slightly larger than $V^{0i,i0}$ for each of the sandwich dimers.

Contrary to the earlier work of Chandross and Ferguson,[5] the later study[118] found no evidence for a heavy-atom effect in the fluorescence yield of the sandwich dimers. This work also failed to measure any triplet emission from any of the sandwich dimers, whereas the phosphorescence of anthracene could be easily detected under the same conditions, and this result was confirmed by Subudhi et al.[119] It was also concluded that the phosphorescence yield of the anthracene sandwich dimer is less than 1% of the yield for anthracene monomer.

Ferguson et al.[118] examined the properties of a number of dissimilar or mixed sandwich dimers obtained from photodissociation of mixed photodimers. These were restricted to a set containing anthracene as one component and the other component being 9-methylanthracene, 9-cyanoanthracene, 9,10-dimethylanthracene, or 9,10-dichloroanthracene.

The features of the mixed sandwich dimers are remarkably similar to those of the symmetrical dimers, which is unexpected because of the large variation in ΔE^1 (from 670 to 1680 cm^{-1}). The intensity distributions and band positions, relative to the component monomer bands, are not those expected on the basis of

simple theory (case 3, II.A.). An example illustrates the difficulty. For (9,10)DMA $\Delta E^1 = 1430$ cm^{-1} and there is nearly an exact resonance between the 0,0 band of the anthracene spectrum and the 0,1 band of the (9,10)DMA spectrum. The positions of the monomer and dimer spectra are as follows:

monomer	dimer
24 950 cm^{-1} (DMA)	24 680 cm^{-1}
26 380 (A, DMA)	26 120
27 800 (A, DMA)	27 490
29 220 (A, DMA)	28 950

The theory (case 3, II.A.) predicts that the 0,0 of (9,10)DMA will be lowered by the sum of the van de Waals shifts and the excitation exchange energy. The 0,0 of anthracene should be raised by the latter and lowered by the former with a net splitting of about 200 cm^{-1}. Contrary to this prediction the separation between the first two maxima is 1440 cm^{-1}, the same as the separation between the two monomer levels, within experimental error. However, the intensity distribution of the dimer spectrum is not the same as the sum of the two monomer spectra, which is inconsistent with a very small interchromophore interaction energy. The other mixed dimer spectra show similar inconsistencies and it seems that the simple theory cannot correctly account for the observations for the states derived from ^1L_a. On the other hand, the absorption spectra of the mixed dimers in the region derived from the ^1B_b state are very similar to those of the symmetrical dimers. Here ΔE^2 is in all cases less than the excitation exchange integrals and the intensities of the two components are expected to be very similar (see Figure 1 for $\mathbf{M}_a^2 \approx \mathbf{M}_b^2$ and $\Delta E^2 < V$) to the symmetric sandwich dimers, as found.

The fluorescence characteristics of the mixed sandwich dimers also provided some problems of interpretation because their emission maxima were similar to the symmetrical dimers and their decay times between 80 and 130 ns compared with about 200 ns for the symmetrical dimers. It was suggested[118] that, in view of the long decay time of excimer emission, some consideration be given to formulating the excimer in terms of the ^1L_b state rather than ^1L_a. More recent work on the spectroscopy of cyclophanes,[120] in particular, has shown that the charge resonance contribution to the dimer states derived from ^1L_b reduces the energy of the lowest two states by at least the same amount as the two lowest states derived from ^1L_a, but it seems more likely that the intrinsic transition moments are reduced in magnitude (see III.E.2.).

Subudhi et al.[116] examined the parentage of the excimer of anthracene by measuring the polarization of the excimer fluorescence. They found that the emission had a positive polarization ratio for irradiation in the ^1L_a band but negative for irradiation in the ^1B_b band, and they concluded that the excimer state is predominantly ^1L_a and not ^1L_b in origin. Curiously they reported a change of polarization across the spectral profile of the emission for polarized absorption at a given wavelength which they attributed to z (parallel to the interchromophore axis) polarization being more important at longer wavelengths. They attributed this z polarization to increased charge-transfer participation at these wavelengths, which is hard to understand because the charge resonance moment for the sandwich dimer involving the ^1L_a molecular state lies in the plane parallel to the short molecular axis.

All of the measurements so far are for sandwich dimers created at 77 K. The emission of the anthracene excimer is green to the eye with a maximum intensity at about 20 400 cm^{-1} and a decay time of about 200 ns. However, if the photodissociation is carried out about 10 K, a red emission with maximum at about 17 400 cm^{-1} and a decay time of 170 ns is also observed.[90] Analogous results were also found for the sandwich dimer of substituted anthracenes and the excitation spectra of the two emissions are different.[91]

Photocleavage of the photodimer of 9,10-dimethylanthracene and tetracene in methylcyclohexane at 77 K and 10 K gave a mixed sandwich dimer with a broad but structured emission which overlapped the absorption spectrum.[121] Unexpectedly, this emission has the relatively long decay time of 60 ns at 77 K whereas the decay time of the relaxed tetracene monomer emission is 8.5 ns. This sandwich dimer needs further investigation, particularly in single crystals. The crystal structure of the photodimer was determined,[121] but its well-developed face is not suitable for discrimination between long- and short-axis polarizations. The photoisomer of 1,3-bis(9-anthryl)propane has the correct morphology, and it should accept the photodimer as a guest. Measurements of absorption and emission from the sandwich dimer were also made in the single crystal of the photodimer at 10 K.[121] Here, the emission spectrum has no structure and there is little or no overlap with the absorption spectrum, so it has the appearance of a mixed excimer or exciplex. The decay time is slightly longer at 85 ns. This overall behavior is very similar to that found for the exciplex between anthracene and naphthalene (III.G.5.).

The ^1L_b state of tetracene should lie relatively much higher than the ^1L_a state than is the case for anthracene, so the long decay time of the exciplex emission from the anthracene–tetracene sandwich dimer is unlikely to involve the ^1L_b state. It appears more likely that the intrinsic transition intensity between the perturbed ^1L_a state of tetracene and the ground state is grossly reduced in the exciplex. For the emission in the crystal this means a factor of 10 which seems enormous. However, there is evidence for the mixed cyclophane between anthracene and naphthalene of a quite marked reduction of the absorption intensity of the anthracene ^1L_a band (III.G.5.). The interpretation of the 200-ns decay time of the anthracene excimer emission as due to cancellation of localized and charge resonance moments, first made by Mataga et al.[122] and generally accepted is no doubt correct, but the intrinsic magnitudes of those transition moments in the excimer are probably considerably smaller than would be estimated from the isolated molecule intensities (III.E.).

Although the reversible photodimerization of anthracene compounds has dominated the sandwich dimer literature, the phenomenon is not limited to these compounds of course. 2-Aminopyridinium salts, acridizinium salts, benzacridinium salts, and 1,3-dimethylthymine form reversible photodimers, and Chandross and co-workers[123] have explored the possible uses of such materials for reversible holographic recording of information. The method involves embedding the photodimers in a transparent matrix. An ultraviolet laser was then used to write a grating pattern into the various samples. Beams having a longer

wavelength could be scattered from these gratings. Unfortunately, various degradation processes limit the image lifetime to unrealistic turn-around times.

Phenanthrene does not form a photodimer but Chandross and Thomas[124] prepared the cis syn dimer of 9-(hydroxymethyl)phenanthrene and prepared a sandwich dimer by photolytic dissociation at 77 K. They did not find excimer emission but rather an excited dimer fluorescence. They also prepared some other substituted phenanthracene photodimers with no evidence of excimer emission from any of the sandwich dimers resulting from them. They did not give any absorption spectra of the sandwich dimers.

Recently Hoshino et al.[125] have reported transient absorption spectra of the anthracene sandwich dimer in 2-methyltetrahydrofuran glass at 77 K. Two time domains were studied, one corresponding to absorption from the singlet excimer and the other from the triplet state. In the former they observed two regions of absorption, one near 12 000 cm^{-1}, the other having peaks at 26 800 and 29 000 cm^{-1}. Hoshino et al.[125] assigned the band at 12 000 cm^{-1} to $^1B_{3g}^- \rightarrow {}^1B_{2u}^-$ and the other group to $^1B_{3g}^- \rightarrow {}^1B_{2u}^+$. Both of these assignments appear to be very doubtful as the observed energies are far too high. With the excimer state at about 20 000 cm^{-1} both of the assigned states should lie within 5000 cm^{-1} above that of the excimer, so they are more likely transitions to higher states of the excimer. It is also not certain that Hoshino et al.[125] used a glass sufficiently rigid to trap a strongly overlapped excimer because the fluorescence spectrum they reported shows vibrational structure and the maximum of the broad component is >20 000 cm^{-1}.

C. Sandwich Dimers From Photoisomers

The first report of the formation of sandwich dimers by reversible photodissociation of a photoisomer of two coupled chromophores was given by Chandross and Dempster.[126] This involved the compound 1,3-bis(1-naphthyl)propane which forms a photoisomer by ultraviolet irradiation. Chandross and Dempster[126] dissociated the photoisomer in methylcyclohexane at 77 K and obtained the expected excimer fluorescence. They did not report any details of the absorption spectrum of the sandwich dimer.

Chandross and Schiebel[127] reported the reversible photoisomerization of 1-(9-anthryl)-3-(1-naphthyl)-propane (ANP) and the formation of a mixed anthracene–naphthalene sandwich dimer.[128] Although they observed only a relatively small effect of interchromophore interaction on the absorption spectrum, they found a broadened fluorescence spectrum with poorly developed vibrational structure and a decay time of 33 ns. They estimated a fluorescence yield of 37%, giving an intrinsic decay time of about 100 ns and suggested that the fluorescent state is very different from that of anthracene, possibly a weak charge-transfer state.

ANP was subsquently studied in single crystals of its photoisomer and again in rigid glasses.[92] Preparation of the sandwich dimer by irradiation in methylcyclohexane at 60 K was found to modify the properties of the exciplex emission, indicating relaxation of the dimer prepared at 77 K. The decay time was extended from 40 ns to 80 ns, the emission no longer contained vibrational structure, and the wavelength of maximum intensity increased. The fluorescence yield of the exciplex was found to have the same yield as the open isomer, contrary to the result of Chandross and Schiebel.[128] Measurements were made of the absorption spectrum after formation of the sandwich dimer at 77 K and after softening of the glass. These showed that the ^1B_b states of the two chromophores interact strongly and when these results are combined with later results for the same system, together with the absorption spectra of the anthracene–naphthalene cyclophanes (III.G.5.) a picture of the effect of reducing the interchromophore separation emerges. With increased interaction, both ^1B_b states move to lower energy and the intensity of the anthracene ^1B_b band decreases while that of the naphthalene ^1B_b band increases. The behavior fits case 3 (II.A.) for dissimilar dimers. The lower energy component of the dimer band, which correlates with the ^1B_b state of the anthracene chromophore, has low intensity because the two transition moments effectively cancel.

A further investigation of ANP was undertaken, which included the determination of the crystal structure of the photoisomer.[129] Photodissociation was carried out at 45 K in methylcyclohexane–decalin (1:1) which forms a very hard glass. A fluorescence excitation technique was used to follow the absorption spectrum changes between 45 and 130 K, mentioned in the previous paragraph. A microspectrophotometric technique was used to determine the polarized absorption spectra of single crystals of the photoisomer containing sandwich dimers obtained by photodissociation at 10 K. The resultant spectra contain contributions from a variety of conformations, some of which are photoisomerizable and can be removed by irradiation. This is particularly shown by the large range of different exciplex emission profiles obtained by monochromatic excitation at different wavelengths.

Hayashi et al.[89,130] examined the two compounds 1,2-bis(1-anthryl)ethane and 1,2-bis(9-anthryl)ethane which form photoisomers. On photodissociation of the photoisomers in a rigid glass at 77 K, excimer emission from the sandwich dimers was observed with a maximum at 530 nm. On the other hand the room-temperature solutions of each open compound showed an excimer fluorescence with maximum intensity at 460 nm. The two excimer emissions were assigned to different conformational arrangements of the two chromophores, an overlapped conformation being assigned to the excimer with maximum at 530 nm. The lack of this emission from the room temperature solutions was ascribed to quenching by formation of the photoisomers. This conclusion was supported by other work[131] carried out with 1,2-bis(9-anthryl)ethane in methylcyclohexane–decalin and acetonitrile solutions. It was concluded that the preferred conformation depends on solvent and temperature, with a partially overlapped conformation being favored in acetonitrile, indicating a solvent-induced charge transfer between the two chromophores in their ground states.

The effects of conformational changes on the absorption spectrum of the sandwich dimer of 1,2-bis(9-anthryl)ethane were studied with single crystals of the photoisomer as a host,[132,133] the structure of which was determined by X-ray methods. The wavelength of the photodissociating light is an important factor which

directly controls the local environment of the dissociated molecule through the extent to which the host lattice is disrupted by the presence of the photodissociated molecules.[91] Nearly uniform concentrations of approximately one dissociated molecule per thousand host molecules can be obtained by using a narrow band of wavelengths on the extreme long-wavelength edge of the absorption band of the crystal. The subsequent absorption spectra are then reproducible with different crystals. If more strongly absorbed light is used to effect photodissociation, too high a local concentration of dissociated molecules is produced, the lattice becomes distorted, the dissociated molecules are able to relax, and spectra more closely related to those obtained in rigid glasses are obtained.

It was found that, even under conditions of low sandwich dimer concentration, numbers of species were produced by photodissociation at 10 K, some fluorescent and others nonfluorescent. The latter could be easily removed by irradiation, but the fluorescent dimers were also photoisomerizable at a much slower rate. The nonfluorescent dimers were ascribed[133] to nearly overlapped conformations with nonplanar anthracene chromophores as their absorption spectra are similar to those of [2.2](9,10)anthracenophane and [2.3]-(9,10)anthracenophane. The fluorescent dimers have absorption spectra, which indicate that the anthracene chromophores are not parallel; i.e., there is an opening of the face to face contact of the chromophores about the ethane bridge.

The analysis of the absorption spectra was materially assisted by the fortunate morphology of the crystals which have two well-developed faces, one of which allows a clear discrimination between short and long axis polarized transitions. The effect of irradiation by strongly absorbed light during the process of photodissociation was also examined, and excitation spectra and narrow band exciting light were used to identify relaxed species. Two relaxed species were identified by their polarized absorption spectra with likely conformations having partially overlapped chromophores.[133] A third relaxed conformation has a structured fluorescence spectrum.

The apparently small difference between the rotated and translated conformations of [2.2](9,10)-anthracenophane produces a profound effect on the spectral features of their absorption spectra as discussed in III.E.4. Similar effects have been found for the sandwich dimer of 1,3-bis(9-anthryl)propane (APA) generated by photodissociation of single crystals of its photoisomer (APAPI).[94] The monoclinic crystal structure of the latter compound has been determined,[94,99] and it has a complex structure with six molecules per unit cell. Four of these molecules are symmetrically related in general positions and are ordered with respect to the orientation of the bridge. The other two symmetrically located molecules are each located on centers of symmetry. Since the APAPI molecule lacks inversion symmetry, it is implied that these latter sites are disordered and randomly occupied by APAPI molecules in either of two orientations.

Closer examination of the crystal structure of APAPI shows that there is a significant difference between the environments of the two molecules.[94] The closer atom–atom contacts of the ordered site suggest that a photodissociated APAPI molecule (APAPI → APA) in this site would be more constrained by the surrounding molecules than would be the case for photodissociation of APAPI molecules in the disordered site.

Since the conformations available to a cleaved APA molecule are essentially predetermined by the crystal cage, a force field optimization procedure was used to predict the conformations of APA as controlled by the constraints of each crystal site. These calculations provided two symmetrical overlapped conformations for the ordered site and a translated conformation in the disordered site. The latter calculated conformation has a C(10)···C(10′) contact of 3.41 Å compared with 2.84 and 3.02 Å for the former two conformations.

Photodissociations of single crystals were carried out about 8 K with weakly absorbed monochromatic light to minimize the disruptive effects of photodissociation on the lattice. The resulting APA molecules with sandwich dimer conformations proved to be nonfluorescent and photoisomerizable (to re-form APAPI) at 8 K. One set of APA molecules could be removed photochemically about 8 times faster than the other group. This more labile set was assumed to occupy the ordered sites, the observed polarizations of its absorption spectrum being consistent with this assignment. The two well-developed crystal faces enabled a discrimination between short- and long-axis polarizations.

The absorption spectrum of the APA in the ordered site bears a resemblance to the rotated conformations of the [2.*n*](9,10)anthracenophanes,[131] while the spectrum of the APA in the disordered site is similar to the spectrum of the translated conformation of [2.2]-(9,10)anthracenophane.[95] These results then underline the conclusions reached from an analysis of the absorption spectra of the various anthracenophanes (III.E.) relating to the effect of overlap on the charge-transfer transition intensity.

V. Concluding Remarks

The spectroscopic data for the various cyclophanes have provided a consistent picture of what happens when two aromatic chromophores are squeezed together in a sandwich configuration, even though the data largely involve measurements in liquid solution and therefore lack spectral detail. This is because of the large variety of cyclophanes which have been made, particularly involving the same chromophores linked at different positions, so that the importance of overlap can easily be seen.

The absorption spectra of the symmetrical cyclophanes require the consideration of two types of states. One correlates with the localized excitation of a single chromophore, while the second corresponds to the transfer of an electron from one chromophore to the other. It appears that it is the second type of state which is more sensitive to the overlap between the two charge distributions, through variation in the coulombic contribution to its energy and through changes in its associated transition intensity. The simplest absorption spectra are associated with that configuration, when there is more than one structural isomer, which has the largest overlap of the two charge distributions. If there is only one structural isomer, then it is the conformation with largest overlap which has the simplest spectrum. These spectra appear simple because the dimer exci-

tation and charge resonance moments, which have comparable magnitudes, tend to cancel for the out-of-phase configurationally interacting states of the dimer if the overlap is large. If the overlap is poor, the charge resonance moment is smaller than the excitation resonance moment and this cancellation does not occur, so all formally allowed transitions are observed.

Although apparently successful assignments of the absorption bands of symmetrical cyclophanes can be made on the basis of interacting chromophores, all of the spectra show very significant loss of absorption intensity across the whole of the spectral region, indicating important changes in the electron charge distribution in these compounds.

Heterophanes and mixed cyclophanes have absorption spectra which can be assigned using a very simple coupled chromophore model which treats the cyclophane as a pair of interacting chromophores. The interaction is assumed to be the dipole–dipole term, but for purposes of calculation the experimental transition dipoles should be distributed in the chromophores using HMO coefficients. This approach seems to work well for the intense bands, e.g., the ^1B_b states of anthracene and naphthalene, but the evidence so far is not so encouraging for the ^1L_a states. The associated absorption bands display very pronounced reductions of intensity compared with analogous monomer chromophores, and the corresponding fluorescence decay times are appreciably lenghtened.

The Stokes shifts of the fluorescence spectra of emitting [2.2]cyclophanes are in all cases small, indicating that the interchromophore separations do not decrease much further in the excimer. The energy of the excimer state is controlled by the overlap between the two chromophores through the energy of the charge-transfer state and its interaction with the related excitation resonance state.

The emitting states of mixed excimers, such as naphthalene–anthracene, appears to have little or no charge-transfer character, as judged by the polarization of the lowest absorption bands. The increased decay times, relative to the isolated chromophore value, are the result of changes in electron distribution which lower the transition moments in both absorption and emission.

The absorption spectra of sandwich dimers made from photodimers and photoisomers are intermediate between those of the isolated chromophore spectra and the spectra of the corresponding cyclophanes, as expected.

There is a need to carry out theoretical calculations of the electronic structures of cyclophanes, particularly with regard to structural isomerism and conformational geometries, in order to understand the reasons for the large absorption intensity reductions which are characteristic of all cyclophane spectra.

VI. Acknowledgments

A number of colleagues have contributed to my 20-year interest in sandwich dimers and cyclophanes. A special debt is owed to Ed Chandross for sharing his original and creative ideas about sandwich dimers. My postdoctoral colleagues Albert Mau, Masaharu Morita, Albert Dunand, and Ray Robbins and former students John Morris, Stanley Miller, and Gerard Wilson have ensured a steady flow of new ideas and experiments. Ray Robbins in particular provided powerful computer programs which have been invaluable. Finally, all of the compounds used in my laboratory have been prepared by Miroslav Puza whose synthetic genius has provided the complete answer to an experimental spectroscopist's prayers.

Note Added in Proof. Two additional papers are relevant to the origin of the long axis polarized absorption band of cyclophanes containing one or two anthracene chromophores (see III.E.3). The study of Steiner and Michl (*J. Am. Chem. Soc.* **1978**, *100*, 6861) used MCD to reassign the earlier work of Michl et al. (ref 54) and the long axis polarized absorption was assigned to ^1L_b. More recently, Zgierski (*J. Chem. Phys.* **1985**, *83*, 2170) has argued that the change of sign observed by Steiner and Michl involves an interference phenomenon (non-Condon terms) involving a totally symmetric vibration of the anthracene chromophore. The absorption spectra of the cyclophanes tend to favor the assignment of the long axis polarized absorption intensity to the ^1L_b state as advanced by Steiner and Michl, although the constant separation of about 1500 cm^{-1} between short and long axis polarized bands in all spectra is particularly difficult to understand. The author thanks A. V. Bree and J. Michl for drawing his attention to these papers.

VII. References

(1) Chandross, E. A.; Ferguson, J. *J. Chem. Phys.* **1966**, *45*, 397.
(2) Chandross, E. A. *J. Chem. Phys.* **1965**, *43*, 4175.
(3) Chandross, E. A.; Ferguson, J.; McRae, E. G. *J. Chem. Phys.* **1966**, *45*, 3546.
(4) Fulton, R. L.; Gouterman, M. *J. Chem. Phys.* **1964**, *41*, 2280.
(5) Chandross, E. A.; Ferguson, J. *J. Chem. Phys.* **1966**, *45*, 3554.
(6) Ferguson, J. *J. Chem. Phys.* **1966**, *44*, 2677.
(7) Stevens, B. *Spectrochim. Acta* **1962**, *18*, 439.
(8) Tanaka, J. *Bull. Chem. Soc. Jpn.* **1963**, *36*, 237.
(9) Ferguson, J. *J. Chem. Phys.* **1958**, *28*, 765.
(10) Stevens, B.; Hutton, E. *Nature (London)* **1960**, *186*, 1045.
(11) Birks, J. B. *Rep. Prog. Phys.* **1975**, *38*, 903.
(12) Foerster, T.; Kasper, K. *Z. Phys. Chem. (Munich)* **1954**, *1*, 275.
(13) Brown, C. J.; Farthing, A. C. **1949**, *164*, 915.
(14) Craig, D. P. *J. Chem. Soc.* **1955**, 2302.
(15) Craig, D. P.; Hobbins, P. C. *J. Chem. Soc.* **1955**, 539.
(16) Reilingh, D. N. de V.; Rettschinck, R. P. H.; Hoytink, G. J. *J. Chem. Phys.* **1971**, *54*, 2722.
(17) Lami, H.; Laustriat, G. *J. Chem. Phys.* **1968**, *48*, 1832.
(18) Rhodes, W. *J. Am. Chem. Soc.* **1961**, *83*, 3609.
(19) Tinoco, I. *J. Chem. Soc.* **1960**, *82*, 4785.
(20) McLachlan, A. D.; Ball, M. A. *Mol. Phys.* **1964**, *8*, 581.
(21) Hida, M.; Sanuki, T. *Bull. Chem. Soc. Jpn.* **1970**, *43*, 2291.
(22) Hirschfelder, J. O.; Curtiss, C. F.; Bird, R. B. *Molecular Theory of Gases and Liquids*; Wiley: New York, 1954.
(23) Craig, D. P.; Thirunamachandran, T. *Proc. Phys. Soc.* **1964**, *84*, 781.
(24) Murrell, J. N.; Tanaka, J. *Mol. Phys.* **1964**, *7*, 363.
(25) Morris, J. M. Ph.D. Thesis, University of Sydney, 1972.
(26) Simpson, W. T.; Peterson, D. L. *J. Chem. Phys.* **1957**, *26*, 588.
(27) Fulton, R. L.; Gouterman, M. *J. Chem. Phys.* **1961**, *35*, 1059.
(28) Gouterman, M. *J. Chem. Phys.* **1965**, *42*, 351.
(29) McRae, E. G. *Aust. J. Chem.* **1961**, *14*, 329.
(30) McRae, E. G. *Aust. J. Chem.* **1961**, *14*, 344.
(31) McRae, E. G. *Aust. J. Chem.* **1961**, *14*, 354.
(32) McRae, E. G. *Aust. J. Chem.* **1963**, *16*, 295.
(33) McRae, E. G. *Aust. J. Chem.* **1963**, *16*, 315.
(34) Witkowski, A.; Moffitt, W. *J. Chem. Phys.* **1960**, *33*, 872.
(35) Kasha, M. *Radiat. Res.* **1963**, *20*, 55.
(36) Merrifield, R. E. *Radiat. Res.* **1963**, *20*, 154.
(37) Bierman, A. *J. Chem. Phys.* **1966**, *45*, 647.
(38) Siebrand, W. *J. Chem. Phys.* **1964**, *40*, 2223.
(39) Perrin, M. M.; Gouterman, M. *J. Chem. Phys.* **1967**, *46*, 1019.
(40) Longuet-Higgins, H. C. *Adv. Spectrosc.* **1961**, *2*, 429.
(41) Lefebvre, R.; Sucre, M. G. *Int. J. Quantum Chem.* **1967**, *1*, 339.
(42) Sucre, M. G.; Geny, F.; Lefebvre, R. *J. Chem. Phys.* **1968**, *49*, 458.

(43) Sucre, M. G. *Int. J. Quantum Chem.* **1969**, *3*, 377.
(44) Young, J. M. *J. Chem. Phys.* **1968**, *49*, 2566.
(45) Koutecky, J.; Paldus, J. *Collect. Czech. Chem. Commun.* **1962**, *27*, 599; **1963**, *28*, 1110, 2667.
(46) Koutecky, J.; Paldus, J. *Tetrahedron Suppl.* **1963**, *19*, 201.
(47) Konijnenberg, E. Doctoral Thesis, Free University of Amsterdam, 1963.
(48) Azumi, T.; McGlynn, S. P. *J. Chem. Phys.* **1964**, *41*, 3131.
(49) Azumi, T.; Armstrong, A. T.; McGlynn, S. P. *J. Chem. Phys.* **1964**, *41*, 3839.
(50) Azumi, T.; McGlynn, S. P. *J. Chem. Phys.* **1965**, *42*, 1675.
(51) Vala, M. T.; Hillier, I. H.; Rice, S. A.; Jortner, J. *J. Chem. Phys.* **1966**, *44*, 23.
(52) Pawlikowski, M.; Zgierski, M. Z. *J. Chem. Phys.* **1982**, *76*, 4787.
(53) Zgierski, M. Z.; Pawlikowski, M. *J. Chem. Phys.* **1983**, *79*, 1616.
(54) Michl, J.; Thulstrup, E. W.; Eggers, J. H. *Ber. Bunsenges. Phys. Chem.* **1974**, *78*, 575.
(55) Cram, D. J.; Allinger, N. L.; Steinberg, H. *J. Am. Chem. Soc.* **1954**, *76*, 6132.
(56) Cram, D. J.; Steinberg, H. *J. Am. Chem. Soc.* **1951**, *73*, 5691.
(57) McClure, D. S. *Can. J. Chem.* **1958**, *36*, 59.
(58) Ingraham, L. L. *J. Chem. Phys.* **1950**, *18*, 988.
(59) Ingraham, L. L. *J. Chem. Phys.* **1957**, *27*, 1228.
(60) Ron, A.; Schnepp, O. *J. Chem. Phys.* **1962**, *37*, 2540.
(61) Ron, A.; Schnepp, O. *J. Chem. Phys.* **1966**, *44*, 19.
(62) Brown, C. J. *J. Chem. Soc.* **1953**, 3265.
(63) Lonsdale, K.; Milledge, J. H.; Krishna Rao, K. V. *Proc. R. Soc. London A* **1960**, *A255*, 82.
(64) Hope, H.; Bernstein, J.; Trueblood, K. N. *Acta Crystallogr., Sect. B: Struct. Crystallogr. Cryst. Chem.* **1972**, *B28*, 1733.
(65) Iwata, S.; Fuke, K.; Sasaki, M.; Nagakura, S.; Otsubo, T.; Misumi, S. *J. Mol. Spectrosc.* **1973**, *46*, 1.
(66) Fuke, K.; Nagakura, S. *Bull. Chem. Soc. Jpn.* **1975**, *48*, 46.
(67) Fuke, K.; Nagakura, S.; Kobayashi, T. *Chem. Phys. Lett.* **1975**, *31*, 205.
(68) Gleiter, R. *Tetrahedron Lett.* **1969**, 4453.
(69) Hoffmann, R. *Acc. Chem. Res.* **1971**, *4*, 1.
(70) Heilbronner, E.; Yang, Z. *Top. Curr. Chem.* **1983**, *115*, 1.
(71) Matsui, K.; Nishi, N.; Kinoshita, M.; Nagakura, S. *Chem. Phys.* **1978**, *35*, 111.
(72) Vala, M. T.; Haebig, J.; Rice, S. A. *J. Chem. Phys.* **1965**, *43*, 886.
(73) Otsubo, T.; Kitasawa, M.; Misumi, S. *Bull. Chem. Soc. Jpn.* **1979**, *52*, 1515.
(74) Pellegrini, M. *Recl. Trav. Chim. Phys-Bas* **1899**, *18*, 457.
(75) Brown, C. J. *J. Chem. Soc.* **1953**, 3287.
(76) Sato, S.; Akabori, S.; Kainosho, M.; Hata, K. *Bull. Chem. Soc. Jpn.* **1966**, *39*, 856; **1968**, *41*, 218.
(77) Griffin, R. W.; Coburn, R. A. *J. Am. Chem. Soc.* **1967**, *89*, 4638.
(78) Allinger, N. L.; Da Rooge, M. A.; Hermann, R. B. *J. Am. Chem. Soc.* **1961**, *83*, 1974.
(79) Shizuka, H.; Ogiwara, T.; Morita, T. *Bull. Chem. Soc. Jpn.* **1975**, *48*, 3386.
(80) Otsubo, T.; Kitasawa, M.; Misumi, S. *Bull. Chem Soc. Jpn.* **1979**, *52*, 1515.
(81) Hefelinger, D. T.; Cram, D. J. *J. Am. Chem. Soc.* **1971**, *93*, 4754.
(82) Froines, J. R.; Hagerman, P. *J. Chem. Phys. Lett.* **1969**, *4*, 135.
(83) Yoshinaga, M.; Otsubo, T.; Sakata, Y.; Misumi, S. *Bull. Chem. Soc. Jpn.* **1979**, *52*, 3759.
(84) Blank, N. E.; Haenel, M. W. *Chem. Ber.* **1981**, *114*, 1531.
(85) Golden, J. H. *J. Chem. Soc.* **1961**, 3471.
(86) Umemoto, T.; Otsubo, T.; Sakata, Y.; Misumi, S. *Tetrahedron Lett.* **1973**, 593.
(87) Iwama, A.; Toyoda, T.; Otsubo, T.; Misumi, S. *Tetrahedron Lett.* **1973**, 1725.
(88) Iwama, A.; Toyoda, T.; Yoshida, M.; Otsubo, T.; Sakata, Y.; Misumi, S. *Bull. Chem. Soc. Jpn.* **1978**, *51*, 2988.
(89) Hayashi, T.; Mataga, N.; Sakata, Y.; Misumi, S.; Morita, M.; Tanaka, J. *J. Am. Chem. Soc.* **1976**, *98*, 5910.
(90) Ferguson, J.; Mau, A. W-H. *Mol. Phys.* **1974**, *27*, 377.
(91) Ferguson, J.; Miller, S. E. H. *Chem. Phys. Lett.* **1975**, *36*, 635.
(92) Ferguson, J.; Mau, A. W-H.; Puza, M. *Mol. Phys.* **1974**, *28*, 1457.
(93) Morita, M.; Kishi, T.; Tanaka, M.; Tanaka, J.; Ferguson, J.; Sakata, Y.; Misumi, S.; Hayashi, T.; Mataga, N. *Bull. Chem. Soc. Jpn.* **1978**, *51*, 3449.
(94) Dunand, A.; Ferguson, J.; Robertson, G. B. *Chem. Phys.* **1980**, *53*, 215.
(95) Dunand, A.; Ferguson, J.; Puza, M.; Robertson, G. B. *Chem. Phys.* **1980**, *53*, 225.
(96) Dunand, A.; Ferguson, J.; Puza, M.; Robertson, G. B. *J. Am. Chem. Soc.* **1980**, *102*, 3524.
(97) Ferguson, J.; Morita, M.; Puza, M. *Chem. Phys. Lett.* **1977**, *49*, 265.
(98) Wada, A.; Tanaka, J. *Acta Crystallogr. Sect. B: Struct. Crystallog. Cryst. Chem.* **1977**, *B33*, 355.
(99) Umemoto, T.; Satani, S.; Sakata, Y.; Misumi, S. *Tetrahedron Lett.* **1975**, 3159.
(100) Mitchell, R. H.; Carruthers, R. J.; Zwinckels, J. C. M. *Tetrahedron Lett.* **1976**, 2585.
(101) Irngartinger, H.; Kirrstetter, R. G. H.; Krieger, C.; Rodewald, H.; Staab, H. A. *Tetrahedron Lett.* **1977**, 1425.
(102) Staab, H. A.; Kirrstetter, R. G. H. *Liebigs Ann. Chem.* **1979**, 886.
(103) Kai, Y.; Hama, F.; Yasuoka, N.; Kasai, N. *Acta Crystallogr. Sect. B: Struct. Crystallogr. Cryst. Chem.* **1978**, *B34*, 1263.
(104) Staab, H. A.; Riegler, N.; Diederich, F.; Krieger, C.; Schweitzer, D. *Chem. Ber.* **1984**, *117*, 246.
(105) Kawashima, T.; Otsubo, T.; Sakata, Y.; Misumi, S. *Tetrahedron Lett.* **1978**, 5115.
(106) Umemoto, T.; Kawashima, T.; Sakata, Y.; Misumi, S. *Chem. Lett.* **1975**, 837.
(107) Otsubo, T.; Mizogami, S.; Osaka, N.; Sakata, Y.; Misumi, S. *Bull. Chem. Soc. Jpn.* **1977**, *50*, 1858.
(108) Otsubo, T.; Mizogami, S.; Osaka, N.; Sakata, Y.; Misumi, S. *Bull. Chem. Soc. Jpn.* **1977**, *50*, 1841.
(109) Iwama, A.; Toyoda, T.; Otsubo, T.; Misumi, S. *Chem. Lett.* **1973**, 587.
(110) Horvath, G.; Kiss, A. *Spectrochim. Acta Part A* **1967**, *23A*, 921.
(111) Solony, N.; Birss, F. W.; Greenshields, J. B. *Can. J. Chem.* **1965**, *43*, 1569.
(112) Tajiri, A.; Asano, T.; Nakajima, T. *Tetrahedron Lett.* **1971**, 1785.
(113) Ferguson, J.; Robbins, R. J.; Wilson, G. J., to be published.
(114) Ferguson, J.; Puza, M.; Robbins, R. J. *J. Am. Chem. Soc.* **1985**, *107*, 1869.
(115) Morris, J. M. *Mol. Phys.* **1974**, *28*, 1167.
(116) Chandra, A. K.; Sudhindra, B. S. *Mol. Phys.* **1974**, *28*, 675.
(117) Califano, S.; Righini, R.; Walmsley, S. H. *Chem. Phys. Lett.* **1979**, *64*, 491.
(118) Ferguson, J.; Mau, A. W-H.; Morris, J. M. *Aust. J. Chem.* **1973**, *26*, 91.
(119) Subudhi, P. C.; Kanomaru, N.; Lim, E. C. *Chem. Phys. Lett.* **1975**, *32*, 503.
(120) Ferguson, J. *Chem. Phys. Lett.* **1981**, *79*, 198.
(121) Ferguson, J.; Mau, A. W-H.; Whimp, P. O. *J. Am. Chem. Soc.* **1979**, *101*, 2363.
(122) Mataga, N.; Torihashi, Y.; Ota, Y. *Chem. Phys. Lett.* **1967**, *1*, 385.
(123) Tomlinson, W. J.; Chandross, E. A.; Fork, R. L.; Ryde, C. A.; Lamola, A. A. *Appl. Opt.* **1972**, *11*, 533.
(124) Chandross, E. A.; Thomas, H. T. *J. Am. Chem. Soc.* **1972**, *94*, 2421.
(125) Hoshino, M.; Seki, H.; Imamura, M.; Yamamoto, S. *Chem. Phys. Lett.* **1984**, *104*, 369.
(126) Chandross, E. A.; Dempster, C. J. *J. Am. Chem. Soc.* **1970**, *92*, 704.
(127) Chandross, E. A.; Schiebel, A. H. *J. Am. Chem. Soc.* **1973**, *95*, 611.
(128) Chandross, E. A.; Schiebel, A. H. *J. Am. Chem. Soc.* **1973**, *95*, 1671.
(129) Ferguson, J.; Mau, A. W-H.; Whimp, P. O. *J. Am. Chem. Soc.* **1979**, *101*, 2370.
(130) Hayashi, T.; Suzuki, T.; Mataga, N.; Sakata, Y.; Misumi, S. *Chem. Phys. Lett.* **1976**, *38*, 599.
(131) Ferguson, J. *Chem. Phys. Lett.* **1980**, *76*, 398.
(132) Ferguson, J.; Morris, M.; Puza, M. *Chem. Phys. Lett.* **1976**, *42*, 288.
(133) Anderson, B. F.; Ferguson, J.; Morita, M.; Robertson, G. B. *J. Am. Chem. Soc.* **1979**, *101*, 1832.